Cell Reports
Medicine

Article

Arrestin-3-assisted activation of JNK3 mediates dopaminergic behavioral sensitization

Graphical abstract

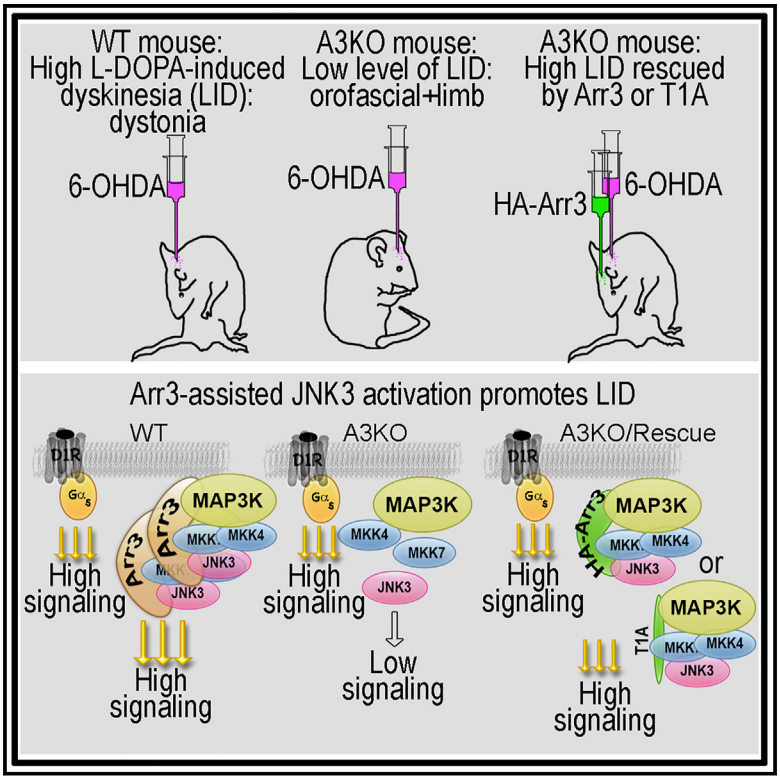

Highlights

- Arrestin-3 knockout mice lack behavioral sensitization to L-DOPA
- Arrestin-3 facilitates activation of JNK3 in the MSNs
- Arrestin-3-assisted activation of JNK3 is required for sensitization
- Arrestin-3-assisted JNK activation is a novel target for anti-dyskinesia therapy

Authors

Mohamed R. Ahmed, Chen Zheng, Jeffery L. Dunning, ..., F. Sanders Pair, Vsevolod V. Gurevich, Eugenia V. Gurevich

Correspondence

eugenia.gurevich@vanderbilt.edu

In brief

Ahmed et al. find that full development of behavioral sensitization to dopaminergic stimulation following a unilateral dopaminergic lesion requires arrestin-3-assisted activation of JNK3 in the striatum. Arrestin-3 acts as a scaffold for the JNK3 pathway in the direct pathway medium spiny neurons promoting the dyskinetic effect of L-DOPA.

Ahmed et al., 2024, Cell Reports Medicine 5, 101623
July 16, 2024
https://doi.org/10.1016/j.xcrm.2024.101623

CellPress

Cell Reports Medicine

CellPress
OPEN ACCESS

Article

Arrestin-3-assisted activation of JNK3 mediates dopaminergic behavioral sensitization

Mohamed R. Ahmed,[1,3,4] Chen Zheng,[1] Jeffery L. Dunning,[2] Mohamed S. Ahmed,[1] Connie Ge,[3] F. Sanders Pair,[4] Vsevolod V. Gurevich,[1] and Eugenia V. Gurevich[1,5,*]

[1]Department of Pharmacology, Vanderbilt University, 2200 Pierce Avenue, PRB422, Nashville, TN 37232, USA
[2]Contet Laboratory, Department of Molecular Medicine, The Scripps Research Institute, La Jolla, CA, USA
[3]University of Massachusetts Medical School, 55 Lake Avenue North, Worcester, MA 01655, USA
[4]The University of Alabama at Birmingham, SHEL 121, 1825 University Boulevard, Birmingham, AL 35294-2182, USA
[5]Lead contact
*Correspondence: eugenia.gurevich@vanderbilt.edu
https://doi.org/10.1016/j.xcrm.2024.101623

SUMMARY

In rodents with unilateral ablation of neurons supplying dopamine to the striatum, chronic treatment with the dopamine precursor L-DOPA induces a progressive increase of behavioral responses, a process known as behavioral sensitization. This sensitization is blunted in arrestin-3 knockout mice. Using virus-mediated gene delivery to the dopamine-depleted striatum of these mice, we find that the restoration of arrestin-3 fully rescues behavioral sensitization, whereas its mutant defective in c-Jun N-terminal kinase (JNK) activation does not. A 25-residue arrestin-3-derived peptide that facilitates JNK3 activation in cells, expressed ubiquitously or selectively in direct pathway striatal neurons, also fully rescues sensitization, whereas an inactive homologous arrestin-2-derived peptide does not. Behavioral rescue is accompanied by the restoration of JNK3 activity, as reflected by JNK-dependent phosphorylation of the transcription factor c-Jun in the dopamine-depleted striatum. Thus, arrestin-3-assisted JNK3 activation in direct pathway neurons is a critical element of the molecular mechanism underlying sensitization upon dopamine depletion and chronic L-DOPA treatment.

INTRODUCTION

Signaling via G protein-coupled receptors (GPCRs) is controlled by a conserved two-step homologous desensitization mechanism: phosphorylation of the active receptors by GPCR kinases and subsequent binding of arrestins, which preclude further G protein coupling.[1] Two non-visual arrestins, arrestin-2 (Arr2) and arrestin-3 (Arr3) (a.k.a. β-arrestin1 and β-arrestin2, respectively), are ubiquitously expressed and negatively regulate the signaling of numerous GPCRs. Arrestins also act as positive regulators of cellular signaling via the assembly of multi-protein complexes.[2–5] The best-known signaling activity of arrestins is to facilitate the activation of the mitogen-activated protein (MAP) kinases ERK and c-Jun N-terminal kinase (JNK).[4,5] Reduced availability of arrestins or their complete elimination results in augmented G protein-mediated responses.[6–8] Mice lacking arrestins also manifest loss-of-function phenotypes, such as blunted behavioral responses to dopaminergic drugs.[9–11] This suggests that arrestin-dependent signaling plays a role in the dopaminergic control of behavior.

Chronic administration of many drugs targeting GPCRs causes long-lasting adaptations. The best-known adaptation is tolerance: the response to the drug diminishes with repeated administration.[12–14] Some drugs also induce the opposite adaptation, called sensitization or reversed tolerance, an enhanced response with repeated use,[12,13,15,16] or cause a paradoxical enhancement of the initial symptoms, as in opioid-induced hyperalgesia.[14] Molecular mechanisms that might underlie tolerance operate in cultured cells, while sensitization is only observed in living animals. Both types of adaptations often coexist *in vivo*, with some drug effects displaying tolerance and others displaying sensitization. Long-term adaptations to drug treatment are a serious clinical problem limiting the efficacy of therapy and/or causing detrimental side effects.

The brain dopaminergic system is critical for the control of motor behavior, reward mechanisms, and cognition. The highest density of dopaminergic innervation and the highest concentration of dopamine (DA) receptors are found in the striatum, a subcortical structure playing an essential role in movement control, motivation, and reward. All five DA receptors are GPCRs and interact with arrestins, although the mode of interaction and its functional consequences are unique for each subtype.[17–22] Long-term use of dopaminergic drugs causes persistent changes in DA-dependent behaviors. In rodents with unilateral ablation of the dopaminergic input to the striatum, stimulation with dopaminergic agonists or the DA precursor L-DOPA causes persistent behavioral and molecular sensitization (reviewed in the study by Bastide et al.[23]). Behavioral sensitization can be

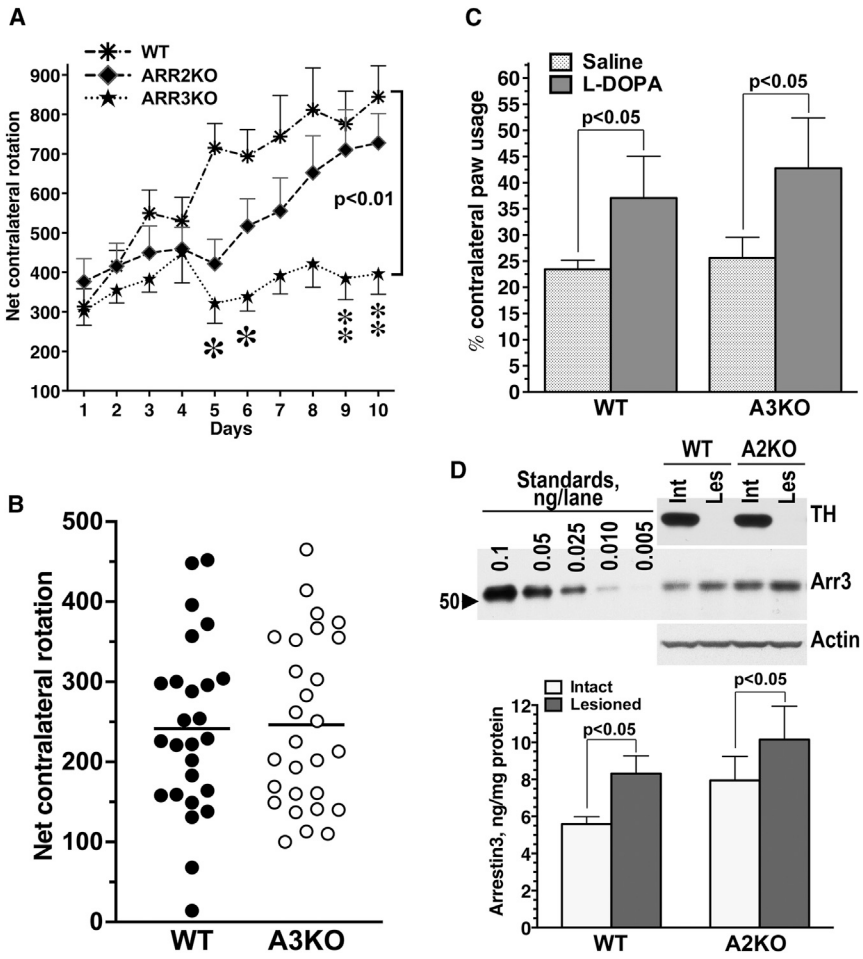

Figure 1. Hemiparkinsonian mice lacking Arr3 (A3KO) respond to dopaminergic stimulation but do not develop behavioral sensitization to L-DOPA

(A) Arrestin-2 knockout (A2KO), A3KO, and WT littermates with unilateral 6-hydroxydopamine lesions were chronically treated with L-DOPA and tested for L-DOPA-induced rotations. Means ± SEM are shown. The statistical comparison was made with respective littermates. WT littermates of A2KO and A3KO were similar. A3KO, but not A2KO, mice demonstrated significantly reduced rotation frequency (genotype effect $F(1,162) = 11.7$, $p = 0.003$, genotype X day $F(9,162) = 3.246$, $p = 0.0012$), indicative of impaired sensitization to L-DOPA. * - $p < 0.05$, ** - $p < 0.01$ by post hoc unpaired Student's t test for individual days.

(B) Apomorphine-induced contralateral rotations (0.1 mg/kg, s.c.) in WT and A3KO mice. The lines show the mean values. No difference was detected.

(C) A3KO and WT mice were tested for forelimb usage in the cylinder test. The mice were injected with saline or L-DOPA (5 mg/kg s.c.) on separate days in a counterbalanced manner. The percentage of contralateral paw usage out of the total is shown. Means ± SEM are shown. The effect of L-DOPA was significant ($p = 0.032$) whereas the effect of genotype was not ($p = 0.89$).

(D) Upper panel: Representative western blot showing the expression of TH in the intact and lesioned striatum in WT and A2KO mice. Lower panel: Quantification of the western blot data demonstrating a significant upregulation of Arr3 in the lesioned hemisphere ($p = 0.0005$). There was no significant difference between WT and A2KO ($p = 0.2$).

elicited in intact animals upon chronic treatment with dopaminergic drugs such as psychostimulants and antipsychotics.[12,13,24–26] The molecular mechanisms of long-term behavioral and signaling plasticity associated with persistent dopaminergic stimulation remain elusive. It is also unclear whether the signaling mechanisms are the same for dopaminergic sensitization of all types, although one common mechanism for some has recently been described.[26]

Here, we show that Arr3 is indispensable for the behavioral sensitization to L-DOPA in mice with unilateral DA depletion and that its action is mediated by the Arr3-dependent activation of JNK in the striatal direct pathway medium spiny neurons (MSNs). This is an excellent mouse model of long-term dopaminergic behavioral plasticity suitable for mechanistic studies of signaling. It is also a widely used animal model of Parkinson's disease (PD). Behavioral alterations caused by L-DOPA in these mice bear an uncanny resemblance to L-DOPA-induced dyskinesia (LID), a side effect of the DA replacement therapy in PD, making it an animal model of LID.[15,23,27–30] Our findings reveal the role of Arr3-dependent JNK activation in the molecular mechanism of sensitization, thereby identifying it as a novel target for anti-LID therapy.

RESULTS

Loss of Arr3 suppresses behavioral sensitization to L-DOPA

The unilateral 6-hydroxydopamine (6-OHDA) lesion of the medial forebrain bundle in rodents results in the massive loss of dopaminergic neurons, particularly in the substantia nigra pars compacta providing dopaminergic innervation of the striatum ipsilateral to the lesion, although the ventral tegmental area innervating the nucleus accumbens is also affected (Figure S1). Animals with such lesions respond by contralateral rotations to administration of the DA precursor L-DOPA or dopaminergic agonists[23,29] and demonstrate multiple signaling adaptations in the lesioned striatum indicative of supersensitivity of striatal neurons.[23,31–33] Chronic treatment of these animals with L-DOPA causes behavioral sensitization and a progressively increased frequency of rotations. We examined sensitization of the L-DOPA-induced rotational behavior in 6-OHDA-lesioned Arr3 knockout (A3KO) and Arr2 knockout (A2KO) mice as compared to wild-type (WT) littermates. A2KO mice showed an initial tendency to reduced rotation frequency but later reached the same level as WT (Figure 1A). In contrast, A3KO mice demonstrated reduced rotations and minimal sensitization to L-DOPA (Figure 1A).

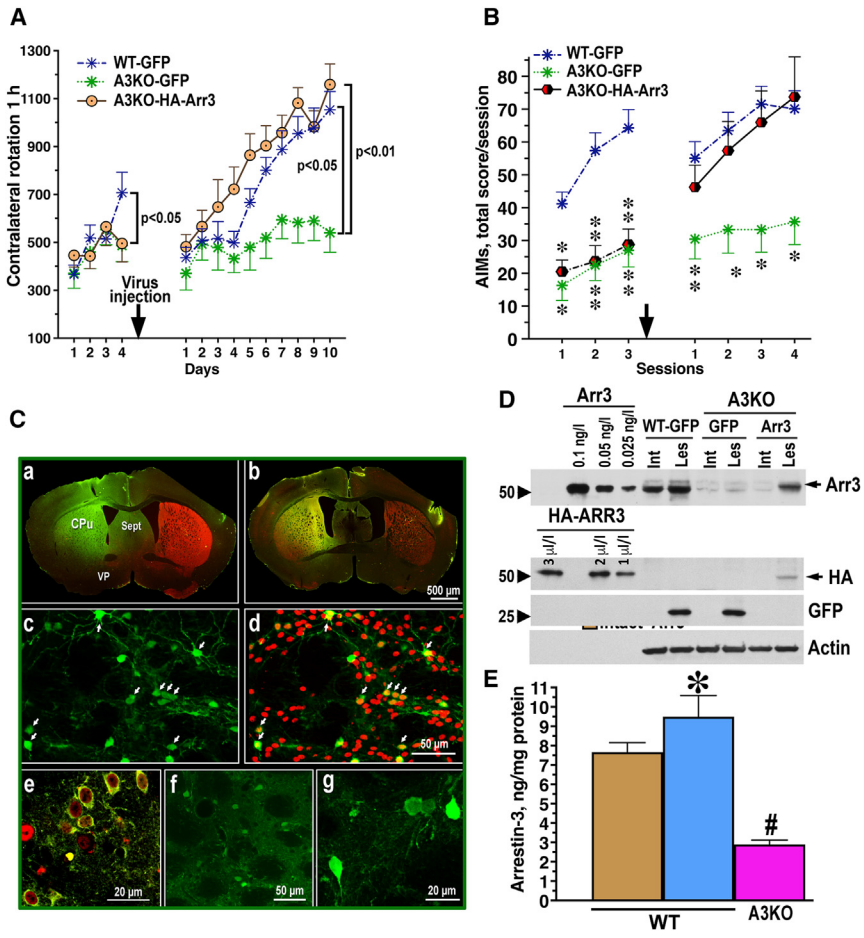

Figure 2. LV-mediated expression of Arr3 in the lesioned striatum rescues L-DOPA-induced rotations and AIMs in A3KO mice

(A) HA-Arr3 rescues rotations in A3KO mice. The LVs were injected into the caudate-putamen (CPu) of A3KO mice. WT mice received GFP. Significance by Bonferroni post hoc test across testing sessions is shown.

(B) HA-Arr3 rescues AIMs in A3KO mice. * - $p < 0.05$, ** - $p < 0.01$ to WT by Dunn's post hoc test following Kruskal-Wallis non-parametric ANOVA.

(C) Protein expression in the lesioned striatum. (a) Low-magnification images of mouse brain. GFP (expressed co-cistronically with Arr3) in the lesioned striatum (green) and TH (red). (b) Low-magnification images of the mouse brain with Arr3 detected by GFP (green) and a marker of MSNs FOXP1 (red). (c, d) Arr3 construct in MSNs labeled with GFP (green) alone (c) or co-localized with FOXP1 (red) (d). Arrows point to co-labeled neurons. (e) High-magnification images of HA-Arr3 in MSNs co-labeled for GFP (green) and FOXP1 (red). (f, g) Low- and high-magnification images of HA-Arr3 labeled with anti-HA antibody (green).

(D) Top: Expression of Arr3 in the intact and infected lesioned striata of WT and A3KO mice infected with GFP or Arr3 LVs. The purified Arr3 served as standards. Bottom: Expression of HA-Arr3 in the lesioned hemisphere of A3KO mice infected with HA-Arr3 LV. Serial dilutions of lysates of HEK293 cells infected with HA-Arr3 LVs were used as standards. Note the absence of HA-Arr3 in WT and A3KO mice infected with GFP and the presence of GFP in both.

(E) Quantification of western blot data. Purified bovine Arr3 served as standards. HA-Arr3 data are absolute numbers in ng per mg of total protein (≈35% of endogenous Arr3 in WT mice). Means ± SEM are shown. * - $p < 0.05$ to the intact striatum; # - $p < 0.001$ to the values in both intact and lesioned striata in WT mice. n = 8–13 mice per group.

A3KO mice were shown to have reduced behavioral sensitivity[9,10] to acute amphetamine. Therefore, the blunted response of A3KO mice to L-DOPA could also reflect an overall lower sensitivity to dopaminergic agents rather than specific signaling adaptation during chronic L-DOPA administration. To test that, we compared locomotor responses to a one-time administration of the DA agonist apomorphine (0.1 mg/kg s.c.) in drug-naive WT and A3KO mice and found them to be similar (Figure 1B). Next, we performed the cylinder test in drug-naive lesioned WT and A3KO mice. Loss of DA upon 6-OHDA lesion reduces the use of the contralateral paw to support the body, whereas L-DOPA supplies DA to the DA-depleted striatum and increases its use. We found that L-DOPA improved the use of the affected paw to a similar extent in WT and A3KO mice, indicating that this acute response to L-DOPA was preserved in A3KO animals not chronically treated with L-DOPA (Figure 1C). Thus, reduced dopaminergic sensitivity, as detected with a different drug (non-selective D2 receptor-preferring agonist apomorphine) and in a different behavioral paradigm (motor cylinder task), does not underlie the L-DOPA sensitization defect of A3KO mice.

We previously detected an upregulation of Arr3 in the affected hemisphere in 6-OHDA-lesioned rats upon chronic L-DOPA treatment.[34] We confirmed this finding in WT mice and found a similar increase in A2KO mice (Figure 1D). A tendency toward upregulation of Arr3 in both hemispheres of A2KO mice, as compared to WT, did not reach statistical significance (Figure 1D). These data suggest that Arr3 is required for sensitization, and its elevated expression upon L-DOPA treatment might contribute to the development of locomotor sensitization to L-DOPA.

Exogenous Arr3 in the striatum rescues behavioral sensitization in A3KO mice

Unilaterally lesioned rodents treated with a high dose of L-DOPA display contralateral rotations, which increase in frequency with each drug administration.[23,32,34,35] Lower doses induce other types of movements collectively referred to as abnormal involuntary movements (AIMs),[28,35] the frequency of which also progressively increases, demonstrating sensitization. The loss of Arr3 reduces sensitization measured by rotations (Figures 1A and 2A) and AIMs (Figure 2B; also see Videos S1 and S2). To

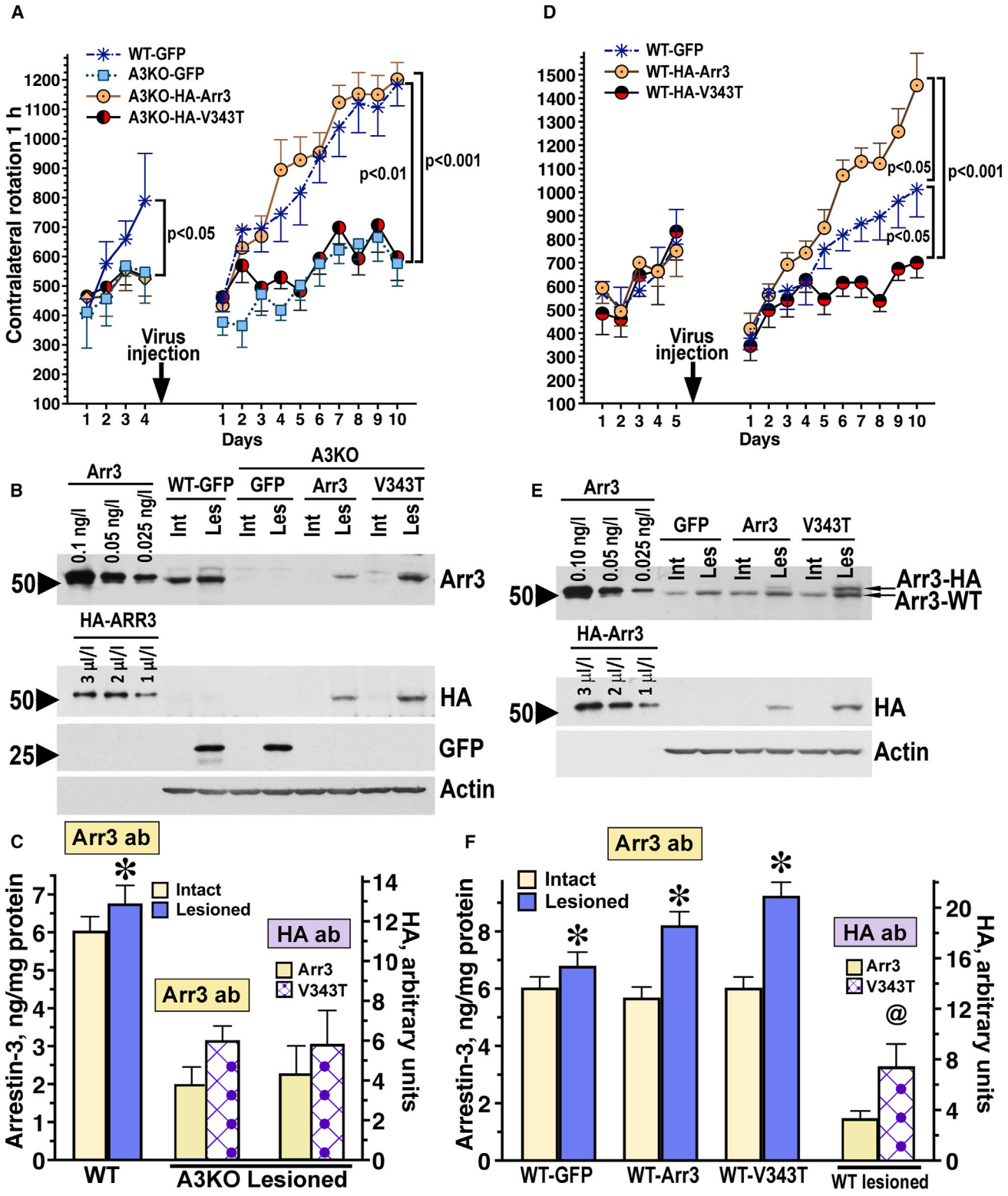

Figure 3. Modulation of L-DOPA-induced rotations by targeting Arr3-dependent JNK activation

(A) The LVs were injected into the CPu of A3KO mice. WT mice received GFP. Expression of HA-Arr3 but not HA-V343T rescued L-DOPA-induced rotations. Significance shown is by Bonferroni's comparison across testing days. For pre-injection testing, the significance applies to comparisons between the WT-GFP

(legend continued on next page)

test whether Arr3 acts during the development of sensitization, we employed a rescue strategy with lentivirus (LV)-mediated gene transfer. LV encoding HA-Arr3 was used to restore Arr3 in the DA-depleted striatum of A3KO mice.

We measured the rotation frequency in mice expressing GFP (control) or Arr3 on the lesioned side in the motor striatum. We pre-tested the mice for 4 consecutive days (Figure 2A). A3KO mice were then randomly assigned to 2 groups that received LVs encoding GFP or Arr3. WT mice expressing GFP served as an outgroup for comparison. During pre-testing, only the WT mice showed sensitization (genotype × day $p = 0.0318$ by repeated measure ANOVA across testing sessions). During the 10-day testing period after LV injection, A3KO mice expressing GFP displayed minimal sensitization, whereas the expression of Arr3 fully rescued the rotational behavior (genotype $p = 0.0022$; genotype X day $p = 0.0019$) (Figure 2A).

Next, we performed a rescue experiment using AIMs as a behavioral readout. During pretesting, A3KO mice demonstrated reduced AIMs compared to WT ($p < 0.001$ by Mann-Whitney test by sessions). In A3KO mice expressing GFP, the level of AIMs remained low. In contrast, the A3KO group expressing Arr3 demonstrated AIMs at a level similar to that of WT mice (group differences significant by Kruskal-Wallis for each session, $p < 0.05$) (Figure 2B). Thus, Arr3 acts during the process of behavioral sensitization.

Postmortem examination showed the expression of HA-Arr3 in the MSNs of the lesioned striatum, as evidenced by co-staining for GFP (expressed co-cistronically with HA-Arr3) with tyrosine hydroxylase (Figure 2Ca) and MSN marker FOXP1 (Figure 2Cb). Western blot with anti-Arr3 and anti-HA antibodies (Figure 2D) showed that LV-encoded HA-Arr3 was expressed at ~30%–37% of the endogenous Arr3 level in the striatum of WT mice (Figure 2E).

Arr3-mediated activation of the JNK pathway is required for its behavioral effect

Arrestins negatively regulate GPCR signaling via homologous desensitization[1] and facilitate signaling via other pathways.[36–38] The loss-of-function phenotype in A3KO mice suggests a loss of Arr3-mediated signaling. Arr3 is the only arrestin subtype that facilitates the activation of JNK family kinases,[39–41] so this pathway seemed a viable candidate. Initially, it was reported that Arr3 selectively activated the JNK3 isoform.[39] We later found that Arr3 also activates JNK1 and JNK2,[42] although JNK3 is its preferred partner.[43,44] To test the role of the JNK pathway in the behavioral function of Arr3, we used the V343T Arr3 mutant with impaired ability to activate JNK.[40] As this was demonstrated in non-neuronal cells, we compared the ability of HA-Arr3 and HA-V343T to facilitate JNK activation in human neuroblastoma SH-SY5Y cells and found that HA-Arr3 increases JNK3 phosphorylation, whereas HA-V343T has minimal effect (Figures S2A and S2B). We compared the ability of HA-Arr3 and HA-V343T to rescue L-DOPA-induced rotations in A3KO mice. HA-Arr3 afforded full rescue ($p < 0.001$ to the GFP group), whereas HA-V343T failed to rescue rotations (Figure 3A) despite comparable expression of both proteins (Figures 3B and 3C).

HA-V343T binds all components of the JNK pathway but fails to activate JNK3.[40] Therefore, we hypothesized that it could have a dominant-negative effect in the presence of endogenous Arr3. In WT mice, we found that HA-Arr3 further enhanced the rotation frequency ($p < 0.05$) (Figure 3D), as compared to GFP control. In contrast, HA-V343T significantly reduced it ($p < 0.05$ to WT-GFP). The behavior of WT mice expressing HA-V343T resembled that of A3KO mice. We detected significantly higher expression of HA-V343T than of HA-Arr3 (Figures 3E and 3F), although the expression of both HA-Arr3 and HA-V343T was much lower than the level of endogenous Arr3 (Figure 3F).

Arr3-mediated activation of JNK in the direct pathway MSNs is sufficient to produce the pro-sensitization effect

The data with HA-V343T suggested that Arr3-dependent JNK activation plays a key role in its pro-sensitization effect. However, Arr3 is a multifunctional protein, and its other functions, which were not tested,[40] might have been altered by the V343T mutation. To specifically test the role of Arr3-dependent JNK activation, we used the monofunctional Arr3-derived peptide T1A that acts as a mini-scaffold facilitating JNK activation in cells[45,46] (Figure S2C). As this has been shown only in non-neuronal cells,[45,46] we ascertained that Venus-T1A facilitated JNK3 activation in human neuroblastoma SH-SY5Y cells, whereas the homologous Arr2-derived peptide B1A did not (Figures S3D and S3E). The expression of Venus-T1A in the lesioned striata of A3KO mice rescued L-DOPA-induced rotations as effectively as full-length Arr3-GFP ($p < 0.001$ to both A3KO-GFP and B1A groups) (Figure 4A). In contrast, Venus-B1A was ineffective (Figure 4A), despite comparable expression of Venus-T1A and Venus-B1A (Figures 4C and 4D).

We also performed a rescue experiment using AIMs as a behavioral readout. During pretesting, A3KO mice demonstrated reduced AIMs compared to WT ($p < 0.001$ by Mann-Whitney test by sessions). In A3KO mice expressing GFP, the level of AIMs remained low, whereas the A3KO group expressing HA-Arr3 demonstrated AIMs at a level similar to that of WT mice (group differences significant by Kruskal-Wallis test, $p < 0.05$ for sessions I and II, $p < 0.001$ for sessions III and IV) (Figure 4B).

group and each of the A3KO groups. Post-injection, $p < 0.001$ applies to the comparison between each of the GFP groups to the A3KO-HA-Arr3 and $p < 0.01$ with the WT-GFP group.

(B) Expression of HA-Arr3 and HA-V343T in the intact and lesioned infected striata. GFP expression and actin (loading control) are also shown.

(C) Quantification of the western blot data. Purified bovine Arr3 was used as standards. * - $p < 0.05$ to the intact striatum by paired Student's t test.

(D) HA-Arr3 increased, whereas HA-V343T significantly reduced, L-DOPA-induced rotations in WT mice.

(E) Detection of endogenous Arr3, HA-Arr3, and HA-V343T (upper panel) and HA-Arr3 (middle panel).

(F) Quantification of the western blot data in the intact and lesioned hemisphere of WT mice infected with LVs encoding HA-Arr3 or HA-V343T. The values in the injected hemisphere (blue bars) reflected the sum of Arr3 plus HA-Arr3 or Arr3 plus HA-V343T. Means ± SEM are shown. $n = 10–13$ mice per group. *, $p < 0.05$ as compared to intact hemisphere; @, $p < 0.05$ as compared to Arr3 by one-way ANOVA.

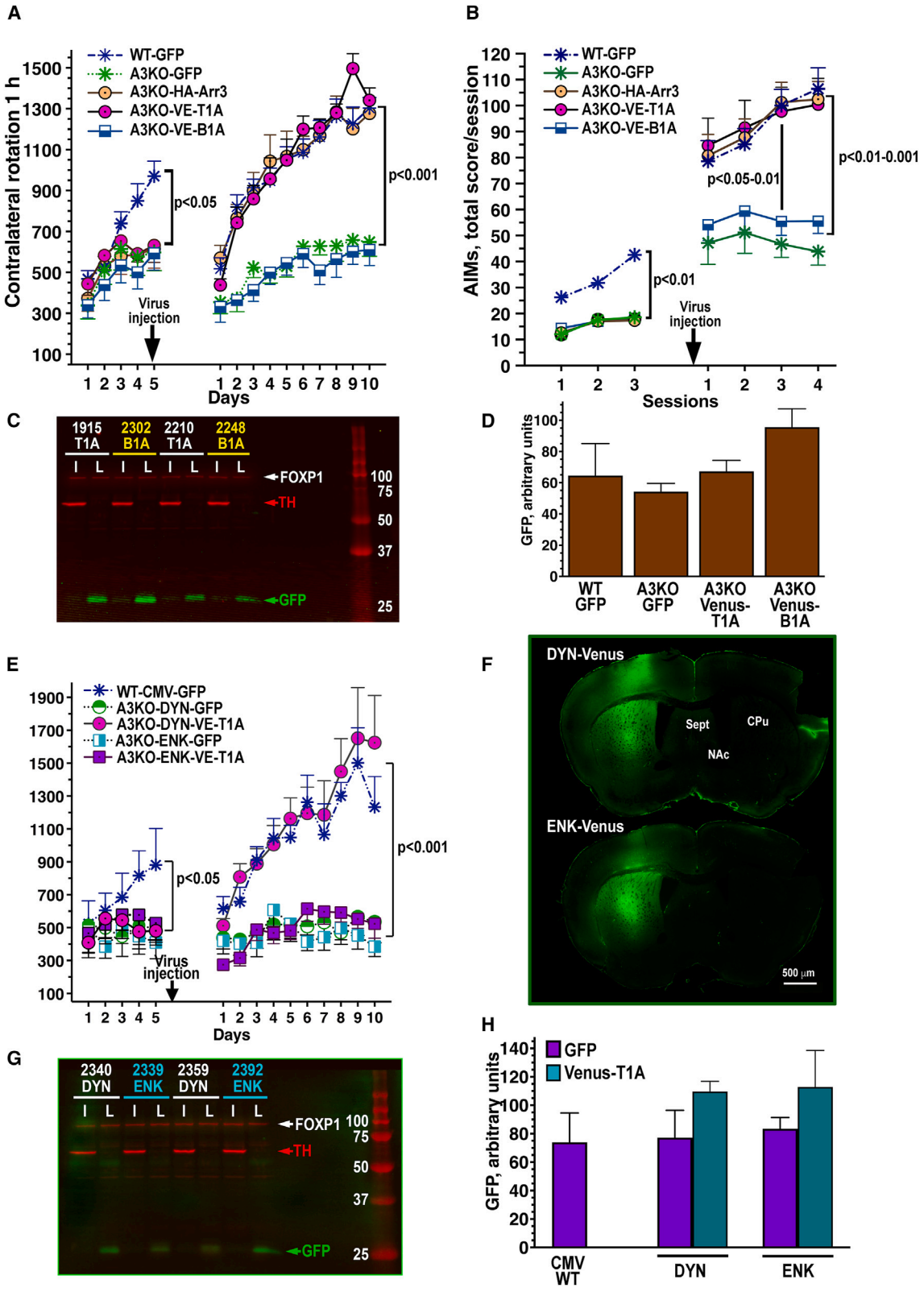

(legend on next page)

Venus-T1A rescued AIMs as effectively as full-length HA-Arr3 (Figure 4B). The analysis of individual AIM scores (Figures S2F–S2H) showed that the lack of Arr3 reduced the frequency of locomotor and axial AIMs (Figures S4G and S4H), whereas their level was high in the groups expressing HA-Arr3 or Venus-T1A. Thus, Arr3 plays a direct role in behavioral sensitization via JNK activation.

The direct and indirect pathway MSNs differ in the expression of the DA receptors and neuropeptides and in their role in movement control.[47,48] The two non-visual arrestins are equally expressed in both types of MSNs.[49] To determine the site of Arr3 action, we constructed LVs with Venus-T1A under the control of cropped dynorphin (DYN) or enkephalin (ENK) promoters to target the expression specifically to the direct or indirect pathway neurons, respectively. These promoters have been used previously.[50] To increase expression, Venus-T1A was placed under the additional control of the internal ribosome entry site (IRES), termed super-IRES for its ability to strongly enhance translation[51] (Figure S3A). These vectors yielded expression comparable to that driven by the strong CMV promoter (Figure S3B). It should be noted that the ENK and DYN promoters used (Figure S3A) cannot be expected to yield the strict specificity of native promoters, which are likely much larger and were not unambiguously defined. However, we showed their neuronal selectivity in the mouse brain by double immunostaining (Figure S3C). We also tested the specificity of DYN and ENK promoters by taking advantage of the differential expression of ENK and DYN in the globus pallidus (GP) and substantia nigra pars reticulata (SNr) (Figure S4). Approximately 40% of GP neurons express ENK but not DYN.[52–55] Conversely, DYN is abundant in the SNr, whereas ENK expression is low or undetectable.[54] We detected ENK promoter-driven GFP expression in GP (Figure S4B) but not in SNr (Figure S4C). In contrast, the DYN promoter drove expression in SNr (Figure S4C) but not in GP (Figure S4B). Thus, the promoters used show significant neuronal specificity.

The expression of Venus-T1A under the control of the ENK promoter did not restore rotations in A3KO mice. In contrast, Venus-T1A expressed under the DYN promoter yielded full rescue ($p < 0.001$ to the DYN-GFP group) (Figure 4E). Both promoters yielded comparable expression in the brain, as evidenced by immunohistochemistry (Figure 4F) and western blot of postmortem samples (Figures 4G and 4H). Thus, the data strongly suggest that Arr3-dependent JNK activation specifically in the direct pathway neurons critically contributes to the dopaminergic behavioral sensitization.

Signaling mechanisms and JNK3 activity in the lesioned striatum

To gain insight into the mechanism of Arr3 action, we tested the activity of signaling pathways known to be altered by persistent treatment with dopaminergic drugs.[9,23,32,35,56] The lesion-induced supersensitivity of the ERK pathway has been implicated in the so-called priming in behavioral sensitization.[23,32,56] Both Arr2 and Arr3 facilitate ERK1/2 activation via scaffolding.[57] We detected the super-responsiveness of ERK1/2 to L-DOPA challenge in the lesioned striatum, but there was no difference between WT and A3KO mice (Figures S5A and S5B). Another MAP kinase, p38, is activated by cellular stresses, like JNKs, and shares many upstream kinases with the JNK pathway.[58] We have previously shown that p38 is activated by L-DOPA challenge in both intact and lesioned striata.[32,56] The degree of p38 activation by L-DOPA was similar in WT and A3KO mice (Figures S5C and S5D). Additionally, the Akt pathway in the DA-depleted striatum becomes constitutively supersensitive following chronic L-DOPA treatment.[32,56] The degree of Akt supersensitivity was also similar in WT and A3KO mice (Figures S5E and S5F).

ERK1/2, JNK1/2/3, and p38 are MAP kinases. MAP kinases are activated by a three-tiered cascade consisting of an MAP kinase kinase kinase (MAP3K), MAP kinase kinase (MAP2K), and output MAP kinase.[59,60] MAP3Ks respond to a large variety of stimuli as shown in Figure S6A for the JNK cascade. MAP kinase signaling is orchestrated by scaffold proteins that organize signaling modules by bringing the kinases of the three levels into close proximity[59] (Figure S6A). While middle-sized MAP2Ks and MAP kinases are turned on by the phosphorylation of the activation loop by upstream kinases, MAP3Ks are large multi-domain proteins, and their mechanisms of activation are very complex and unique for each kinase[59,61–63] (Figure S6A).

Figure 4. Rescue of L-DOPA-induced rotations and AIMs in A3KO mice by the JNK3-activating Arr3-derived peptide T1A

(A) Both HA-Arr3 and T1A, but not the Arr2-derived homologous peptide B1A, rescued L-DOPA-induced rotations in A3KO mice. Significance for post-test applies to pairwise comparisons between WT-GFP and A3KO-T1A with A3KO-GFP and A3KO-B1A by Bonferroni's comparison. Before virus injection, WT was the only group significantly different from the rest.

(B) HA-Arr3 and T1A rescued AIMs in A3KO mice, whereas B1A did not. Note that due to lower AIMs levels in pre-testing, the dose of L-DOPA was increased to 10 mg/kg during post-testing. Post-test significance levels are for pairwise comparisons between each of the groups: WT, A3KO/HA-Arr3, and A3KO/T1A versus each of A3KO/GFP ($p < 0.01$) and A3KO/B1A ($p < 0.05$) by Dunn's post hoc test for each session. The differences in sessions I and II (not shown) are the same as in session III. For pre-test, $p < 0.01$ between WT and all A3KO groups across sessions.

(C) Western blot for Venus-T1A and Venus-B1A (GFP; green) and TH and FOXP1 (red). The blots were visualized with the Odyssey CLX imaging system.

(D) Quantification of the western blot data. There were no significant differences in the expression of the Venus-fused peptides among the experimental groups ($p = 0.22$).

(E) Venus-T1A, expressed in striatonigral MSNs under control of the DYN promoter, rescued rotations in A3KO mice, whereas Venus-T1A in striatopallidal MSNs under control of the ENK promoter did not. Significance shown is by Bonferroni test across all testing sessions. Significance shown after the virus injection applies to pairwise comparisons between WT-GFP and A3KO-DYN-T1A with A3KO-DYN-GFP, A3KO-ENK-GFP, and A3KO-ENK-T1A. Before the virus injection, WT was the only group significantly different from the rest.

(F) Brain sections stained for GFP show the expression driven by the DYN and ENK promoters. Spt, septum; NAC, nucleus accumbens; CPu, caudate-putamen.

(G) The expression of Venus-T1A driven by the DYN and ENK promoters detected by western blot.

(H) Quantification of the western blot data. There were no significant differences in the expression of Venus-T1A among the experimental groups ($p = 0.43$ one-way ANOVA). Means ± SEM are shown. $n = 9–11$ mice per group.

Ten JNK isoforms are expressed in the brain: four splice variants of JNK1, four of JNK2, and two of JNK3 (Figure S6B). Phospho-JNK (ppJNK) is seen as two bands at 54 and 46 kDa (Figure S6C), which contain nine out of the ten known JNK isoforms.[64] In the mouse striatum, in contrast to the rat, the longer JNK3 splice variant JNK3α2 (57 kDa) is undetectable by ppJNK antibody (Figure S6C). The shorter JNK3α1 is the major variant in both rat and mouse striata. It runs at 54 kDa together with two variants of JNK2 (JNK2α2 and JNK2β2) and two variants of JNK1 (JNK1α2 and JNK1β2) (Figure S6C). The lower band contains two shorter JNK2 (JNK2α1 and JNK2β1) and two JNK1 (JNK1α1 and JNK1β1) splice variants.

We tested JNK3 activity in the striata of WT and A3KO mice. The anti-JNK3 antibody precipitated both JNK3 isoforms, and the samples were then immunoblotted for ppJNK (Figures 5A and 5D). We compared the fraction of active JNK3 in the intact and lesioned striata of WT and A3KO mice chronically treated with saline or L-DOPA and challenged with L-DOPA 45 min before sacrifice. We found no differences between the genotypes in the intact hemisphere regardless of the treatment (Figures 5A–5C). In contrast, in the lesioned hemisphere, WT mice had a significantly higher activity of both isoforms of JNK3, particularly of JNK3α2, than A3KO mice (Figures 5A–5C). To test the effect of Arr3 on JNK3 activity in the lesioned striatum, we compared the activity of both JNK3 isoforms in WT mice and A3KO mice injected with LVs encoding GFP (control) or HA-Arr3. In parallel with the behavioral sensitization, exogenous HA-Arr3 rescued the JNK3 activation in A3KO mice (Figures 5D–5F).

The transcription factor c-Jun is the best-known substrate of JNKs,[65] which gave this family of kinases its name (c-Jun N-terminal kinase). JNK-dependent phosphorylation and activation of c-Jun has been studied in the context of the JNK role in apoptosis.[43,64] The role of JNK-c-Jun signaling in neural processes unrelated to cell death is beginning to be appreciated.[64,66] We examined the level of c-Jun phosphorylation in the striata of WT and A3KO mice, both drug-naive animals challenged with L-DOPA and mice chronically treated with L-DOPA. Chronic L-DOPA administration significantly increased the JNK-dependent c-Jun phosphorylation in the DA-depleted striatum in WT but not in A3KO mice (Figures 6A–6C). Phospho-c-Jun was significantly reduced (Figures 6C and 6D) ($p < 0.01$) in the lesioned striatum of chronically L-DOPA-treated A3KO animals as compared to WT. The LV-mediated expression of Arr3 rescued c-Jun phosphorylation (Figures 6D–6F).

Thus, the loss of Arr3 reduced the activity of JNK3 and phosphorylation of c-Jun in the DA-depleted striatum. Arr3 expressed via lentiviral gene transfer rescues both JNK activity and c-Jun phosphorylation in parallel with the behavioral rescue.

Arr3 regulates behavior via scaffolding of the JNK activation cascade

It has been reported previously that Arr3 overexpressed in the lesioned striatum of mice and non-human primates suppresses behavioral sensitization.[67] Our results in A3KO mice appear to contradict this finding. The previous study used adeno-associated viruses (AAVs) as vectors. AAVs are known to induce high expression levels. The JNKs are the output kinases activated by a three-tiered cascade of kinases that sequentially phosphorylate and activate the downstream kinase.[68] We previously showed that Arr3 facilitates JNK activation via simple scaffolding with a bell-shaped curve of the dependence of JNK3 phosphorylation on Arr3.[42,44,69,70] A bell-shaped curve is characteristic of the simple scaffolding mechanism: low scaffold concentrations promote activation, while high concentrations beyond a certain point decrease the output.[71] We confirmed the scaffolding nature of the Arr3-mediated JNK3 activation in neuronal SH-SY5Y cells (Figure S7). Thus, the effect of Arr3, acting as a scaffold *in vivo*, on the JNK activity and behavior likely depends on its concentration. We tested the effect of Arr3 as a function of its expression level. To this end, we compared the effects of the Arr3 gene transfer mediated by AAV and LV on the sensitization of rotations and AIMs in WT mice. We confirmed that the LV-mediated expression of Arr3 in the lesioned striatum of WT mice facilitated locomotor sensitization to L-DOPA (compare Figures 3D and 7A). In contrast, the AAV-mediated expression of Arr3 significantly suppressed sensitization (Figure 7A). The LV and AAV-mediated Arr3 expression in the lesioned striata also produced opposite effects on the frequency of AIMs (Figure 7B). Western blots showed that LV-driven expression was at 30%–35% of the endogenous level (Figures 7C and 7D), as in previous experiments (Figures 2E, 3C, and 3F). In contrast, the AAV-mediated expression exceeded the endogenous Arr3 level in WT mice approximately 10-fold (Figures 7D and 7E).

DISCUSSION

Our main finding is that, after unilateral DA depletion, mice lacking Arr3, but not Arr2, display a reduced propensity for behavioral sensitization by chronic treatment with L-DOPA. Sensitization was measured in two independent tests, contralateral rotations and AIMs. Contralateral rotations are a response to high doses of L-DOPA and DA agonists in mice with unilaterally ablated neurons that provide DA to the striatum. The frequency of these rotations progressively increases upon chronic treatment.[32,34,35,56,72] Lower L-DOPA doses bring about orofacial, locomotor, and trunk movements collectively known as AIMs,[28,73] the frequency of which also increases with each L-DOPA administration. We found that Arr3 is required for sensitization, since A3KO mice do not manifest it, whereas exogenous Arr3 supplied to the striatum via viral gene transfer fully rescued the sensitization of both behaviors. We detected full behavioral rescue with exogenous expression as low as 30%–35% of the endogenous level. This indicates that the concentration of endogenous Arr3 exceeds the level required for behavioral sensitization. We found previously that visual arrestin-1 levels as low as 4%–12% of the endogenous level sufficed to support normal rod photoreceptor function.[74] Considering the multitude of Arr3 functions,[75–77] the fact that a low level of Arr3 is sufficient to sustain sensitization is not surprising. Apparently, even the signal from the subpopulation of neurons where Arr3-assisted JNK activation was restored by exogenous Arr3 triggers a full-scale behavioral response.

We found that Arr3 contributes to the sensitization process via Arr3-assisted activation of the JNK pathway, primarily JNK3. This conclusion is based on the failure of Arr3-V343T, which is

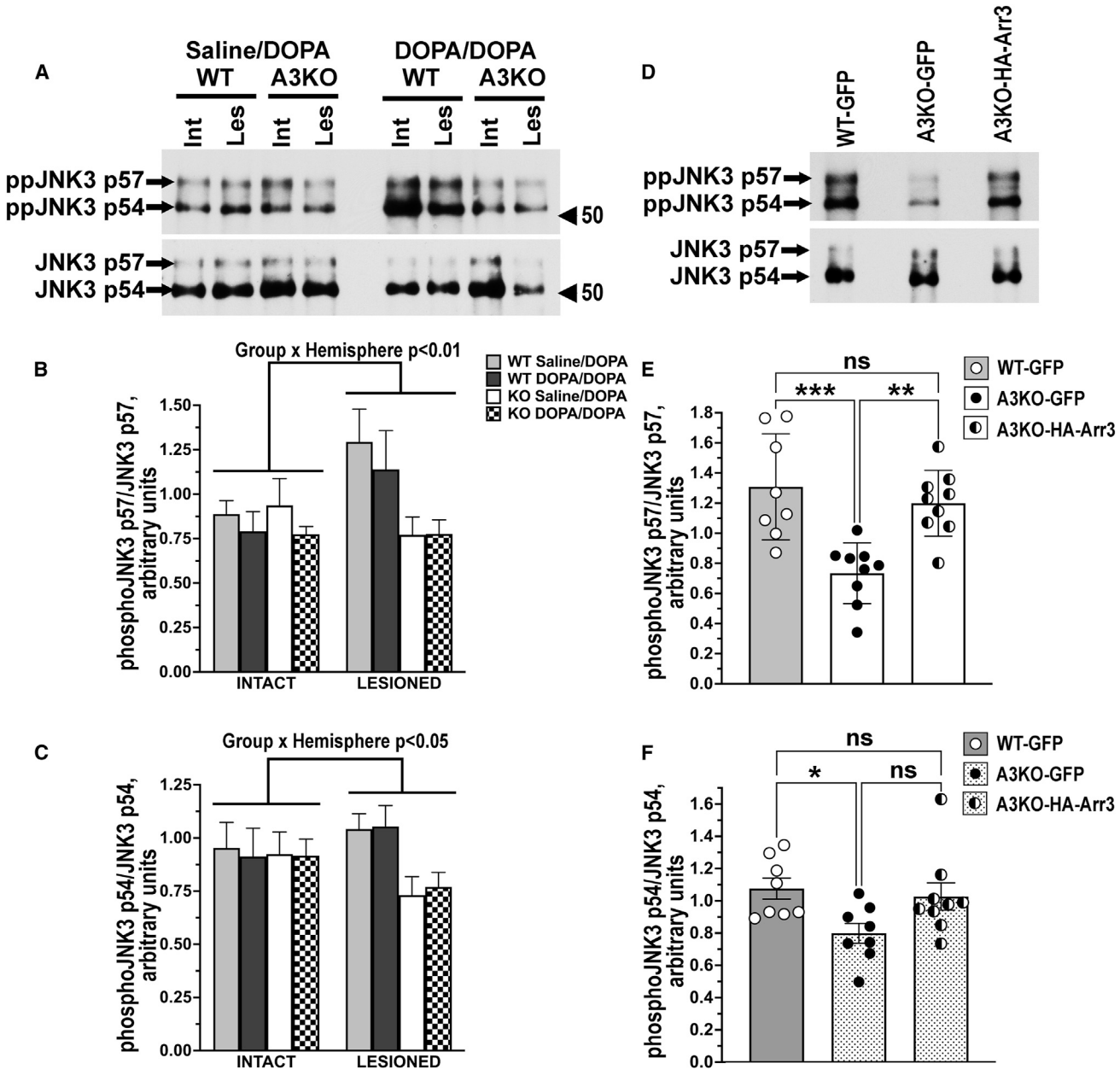

Figure 5. Changes in the activity of JNK3 in the striatum associated with the loss of Arr3

(A) Representative western blots showing phosphorylated JNK3 isoforms (upper panel) and total JNK3 (lower panel) immunoprecipitated from the CPu. Arrows with numbers point to JNK isoforms.

(B) Quantification of the western blots for phospho-JNK3α2 (p57) normalized by total immunoprecipitated JNK3α2 (p57). Two-way repeated measure ANOVA with group and gemisphere yielded significant group × hemisphere interaction ($p < 0.01$). The level of JNK3α2 (p57) phosphorylation in A3KO mice was significantly lower than that in WT mice ($p < 0.05$). $n = 5–7$.

(C) Quantification of the western blot data for phospho-JNK3α1 (p54). The same statistical analysis as for p57 yielded significant group × hemisphere interaction ($p < 0.05$), which is due to enhanced activation of JNK3 p54 in the lesioned hemisphere of WT mice.

(D) Representative western blots showing phosphorylated JNK3 isoforms (upper panel) and the total immunoprecipitated JNK3 (lower panel) in the lesioned striata of WT mice and A3KO mice injected with GFP or HA-Arr3 LV.

(E) Quantification of the western blot data for phosphorylated JNK3α2 (p57) normalized to total immunoprecipitated JNK3α2 (p57). One-way ANOVA yielded highly significant effect of Group ($p = 0.0003$). **$p < 0.01$, *** - $p < 0.001$ by Tukey's post hoc test.

(F) Quantification of the western blot for phospho-JNK3α1 (p54) normalized to total immunoprecipitated JNK3α1 (p54). The effect of group was significant ($p = 0.0324$). * - $p < 0.05$ by Tukey's test. Means ± SEM are shown throughout.

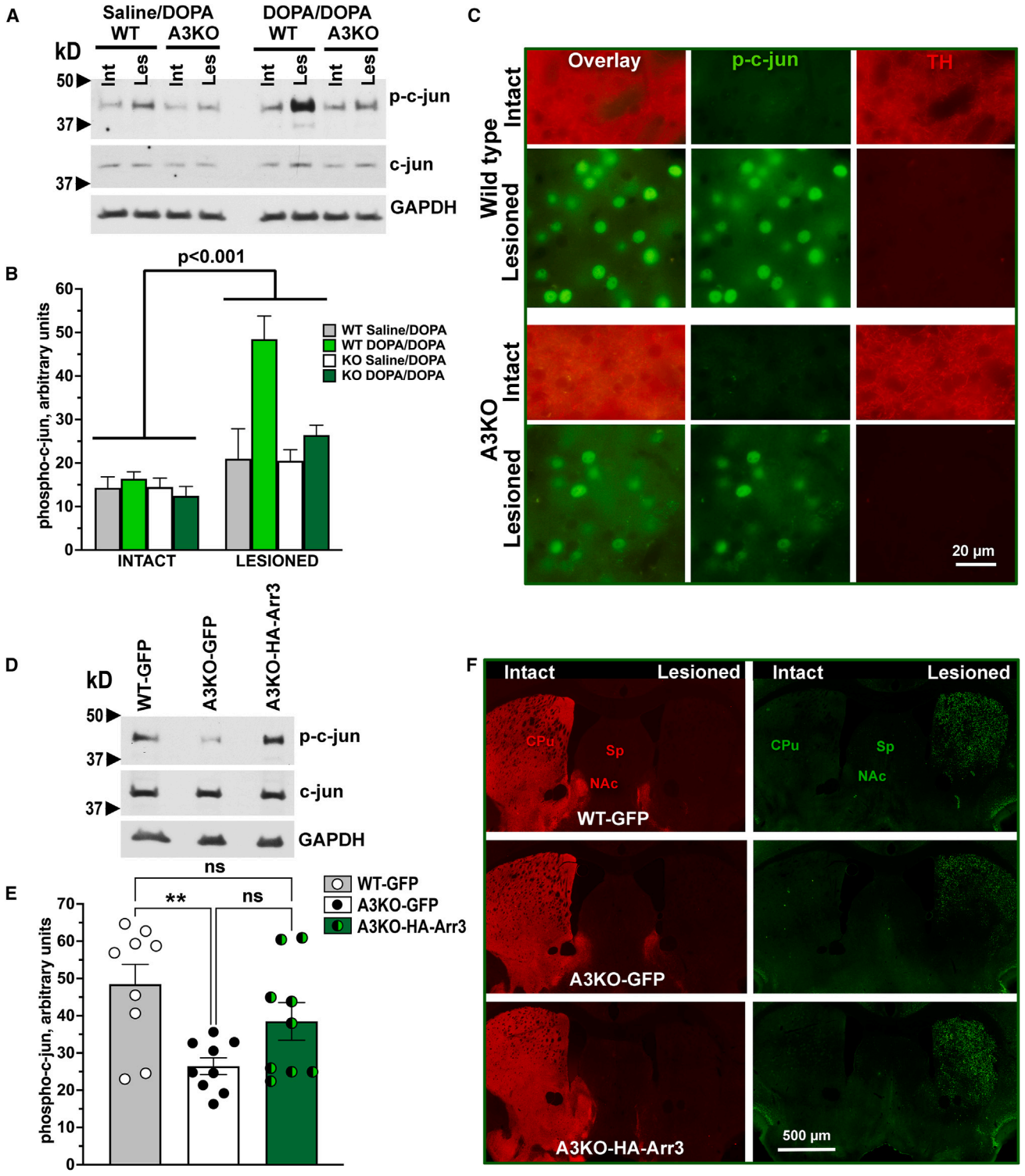

Figure 6. Changes in the JNK-dependent c-Jun activation associated with the loss of Arr3

(A) Representative western blots showing the levels of c-Jun phosphorylated at the JNK site Ser73 (upper panel) and total c-Jun (middle panel).

(B) Quantification of the western blot data for phospho-c-Jun. Significant hemisphere × group interaction ($p < 0.001$) is due to elevated c-Jun phosphorylation in the lesioned striatum of L-DOPA-treated WT mice not evident in other groups. $n = 6–9$.

(C) High power images of the mouse brain double-stained for phospho-c-Jun (green) and TH (red).

(legend continued on next page)

defective in JNK activation, to rescue sensitization and on its ability to inhibit sensitization in WT animals, apparently acting in a dominant-negative manner. Sensitization was rescued in A3KO mice by an Arr3-derived short peptide T1A capable of activating JNK but lacking other functions of the full-length Arr3.[45,46] We detected the expected supersensitivity in A3KO mice of other signaling pathways previously found to be abnormal following DA depletion and/or L-DOPA treatment in WT animals[34,35,51,56] (see also the study by Bastide et al.[23] and references therein). We also detected defective JNK3 activation in A3KO mice, which is rescued by virally delivered Arr3 in parallel with the behavioral rescue. Full rescue by the JNK-activating peptide T1A incapable of interacting with GPCRs rules out the role of the Arr3 action at GPCRs in sensitization. Our data implicate Arr3-assisted JNK3 activation in L-DOPA-induced behavioral plasticity.

Arr2 and Arr3 regulate numerous signaling pathways,[3–5] interacting with >100 proteins each.[77] This is one of very few studies of arrestin-mediated signaling where the exact arrestin-regulated pathway responsible for the biological response in living animals has been identified.[9,78] It is also the first study implicating the JNK pathway in behavioral sensitization to L-DOPA. The activity of the JNK pathway in general and JNK3 in particular is most often regarded in the context of cell death in neurodegenerative disorders.[79–81] However, JNK3 has functions in the brain unrelated to neuronal death.[64,80,82,83]

In WT mice, both JNK activity and JNK-dependent phosphorylation of c-Jun are upregulated by the dopaminergic lesion and/or L-DOPA treatment. In contrast, in A3KO mice both are lacking, implicating Arr3-dependent JNK activation in these effects. However, the connection between reduced c-Jun phosphorylation and the loss of Arr3 and/or reduced JNK3 activity remains tenuous. JNK3 phosphorylates many other transcription factors in the nucleus and dozens of proteins in the cytoplasm.[65,84,85] The data do not exclude the possibility that JNK3 phosphorylation of targets other than c-Jun plays a key role in sensitization. This issue requires further investigation.

Our data suggest that Arr3 acts in the direct pathway MSNs expressing the D1 DA receptor. Although cell type specificity of the cropped DYN and ENK promoters is likely imperfect, the behavioral rescue produced by the expression of T1A under the DYN promoter is remarkable in comparison with the lack of effect when the ENK promoter is used. This strongly suggests that Arr3 acts primarily in the DYN/D1R-expressing MSNs. Numerous studies have demonstrated supersensitivity of D1 receptors brought about by DA depletion, which may or may not be ameliorated by subsequent L-DOPA treatment[35,86–88] (see also the study by Bastide et al.[23] and references therein). Studies of the behavioral manifestations caused by dopaminergic drugs in animals with DA depletion have focused on GPCRs expressed by MSNs, primarily DA receptors (reviewed in the study by Bastide et al.[23]). We found that the lesion-induced supersensitivity of the ERK pathway, which has been reported previously by us[32,56] and others,[30,33,47,87,88] is preserved in A3KO mice. The supersensitivity of p38,[32,56] which is the most closely related to JNKs, and the Akt pathway[32,56] is also preserved in A3KO mice. Selective analysis of JNK3 responsiveness showed that the activity of both JNK3 isoforms is elevated following the 6-OHDA lesion regardless of L-DOPA treatment, and this response is missing in A3KO mice.

The exaggerated ERK response in the lesioned striatum has been attributed to the supersensitivity of D1R.[31,47,87,88] We have previously showed that the lesion-induced D1R supersensitivity is, at least partially, due to defective desensitization because of its insufficient phosphorylation by GRK6,[35] as LV-mediated overexpression of GRK6 in the lesioned striatum suppressed the supersensitive ERK response to L-DOPA and ameliorated behavioral abnormalities,[35,56] likely by facilitating D1R desensitization. Our data suggest that the action of Arr3 in MSNs following DA depletion is unrelated to D1R desensitization. This conclusion seems counterintuitive, since arrestins were initially identified as GPCR-binding proteins negatively regulating G protein-mediated signaling. Even the arrestin-mediated signaling was originally envisioned as a function of GPCR-bound arrestins.[89,90] This is true for the arrestin-dependent regulation of ERK1/2, as only GPCR-bound arrestins have high affinity for ERK[41,62] and facilitate ERK1/2 activation.[62,91] In contrast, there is ample evidence that the JNK pathway is regulated by non-receptor-bound Arr3.[41,45,91–93] This raises the question about a link between the stimulation of DA receptors following L-DOPA administration and Arr3-dependent JNK3 activation.

The dopaminergic activity is indispensable, since without L-DOPA no sensitization is observed. Arr3 serves as a scaffold of the JNK-activating pathway, i.e., it facilitates signal propagation (Figure S7) but does not initiate signaling. In the absence of a relevant activated MAP3K(s), no JNK activation can ensue regardless of the assembly of the MAP3K-MAP2K-MAPK module. Thus, it is tempting to speculate that one or more of the upstream MAP3Ks serves as a link.[59,94] There is so far no evidence that MAP3Ks are directly activated by D1R stimulation. However, one of the MAP3Ks, the dual leucine zipper kinase (DLK), is phosphorylated and activated by protein kinase A (PKA).[95,96] It is conceivable that the supersensitive D1R, by strongly stimulating cyclic AMP production and subsequent PKA activation, could serve as an activator of DLK. Alternatively, indirect activation of select MAP3Ks by cellular stress caused by the high level of DA upon L-DOPA administration could be envisioned. Thus, the activation of one or more upstream MAP3Ks of the JNK pathway might serve as a link between D1R stimulation and Arr3-assisted JNK3 activation. Humans express 20 MAP3Ks.[57,59] Arr3 was shown to bind only one of these, ASK1.[39] It is not known whether it binds any of the others. This issue awaits further investigation.

Arrestins serve as scaffolds of the MAP kinase activation cascades (Figure S7).[5,39,62] This means that arrestins, lacking their own enzymatic activity, facilitate signaling by bringing the

(D) Representative western blots showing phosphorylated and total c-Jun.

(E) Quantification of the western blot data for phospho-c-Jun. One-way ANOVA yielded significant effect of group ($p = 0.007$). ** - $p < 0.01$ by post hoc Tukey's test.

(F) Low power images of sections co-stained for TH (red) and phospho-c-Jun (green).

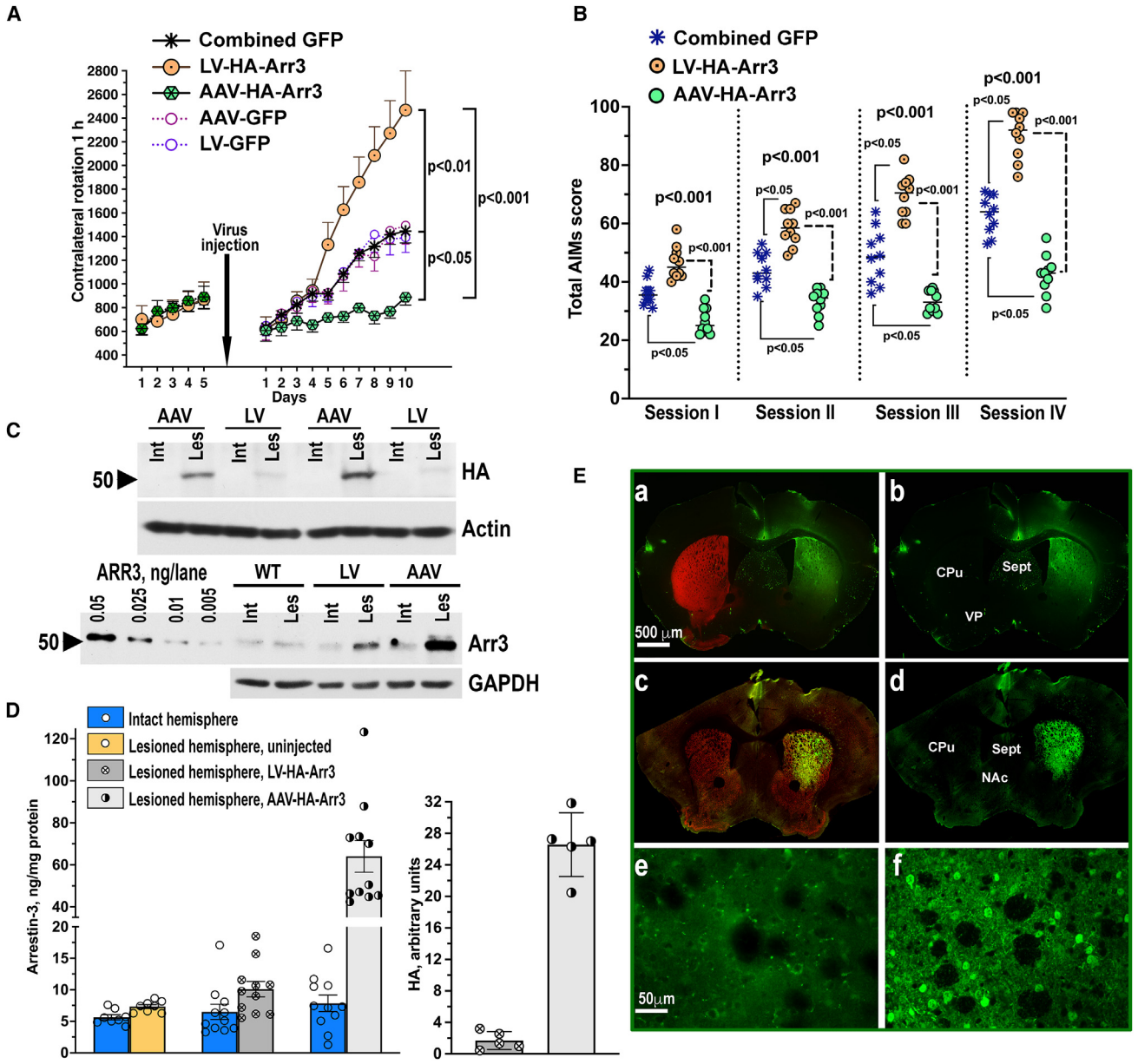

Figure 7. The effects of LV- or AAV-mediated Arr3 expression in WT mice

(A) The expression of HA-Arr3 driven by LV enhanced L-DOPA-induced rotations, whereas the AAV-mediated expression suppressed sensitization (genotype effect $F(2,270) = 17.9$ $p < 0.001$; genotype X day effect $p < 0.001$); the significance shown is by Bonferroni test across days. Means ± SEM are shown.

(B) The graph shows post-test sessions analyzed by Kruskal-Wallis ANOVA (significance levels shown above). The brackets indicate significant differences to WT-GFP group by Dunn's test.

(C) Upper panel: Expression of HA-Arr3 mediated by LV or AAV detected with anti-HA antibody. Actin is shown as loading control. Lower panel: HA-Arr3 detected with anti-Arr3 antibody. Purified Arr3 (four left lanes) served as standards for quantification. Note that endogenous Arr3 and exogenous HA-Arr3 are not resolved on the gel. The AAV sample with the lowest Arr3 expression was used to avoid overexposure. GAPDH is shown as loading control.

(D) Quantification of the western blot data. Scatterplots with means ± SEM are shown. Significance between indicated groups is by Dunn's post hoc test.

(E) Images of the mouse brain. (a, b) A striatal section from a mouse following LV-HA-Arr3 injection co-stained for GFP (green) and TH (red); a, an overlay; b, GFP; (c, d), a striatal section after AAV-Arr3 injection co-stained for GFP (green) and FOXP1 (red); c, an overlay; d, GFP; (e, f), high power images of the sections from the striatum infected with LV-HA-Arr3 (e) or AAV-HA-Arr3 (f) stained for HA. Abbreviations as in Figures 2C and 5B.

kinases into proximity and thus promoting their sequential activation. Mathematical modeling has revealed a biphasic dependence of the signaling effect on the scaffold concentration, with a lower concentration enhancing and a higher concentration inhibiting the signaling.[71,97] This is intuitive: when there are fewer molecules of the scaffold than of the scaffolded kinases, its

presence increases the probability of the assembly of complete multi-kinase signaling modules, whereas when there is more scaffold than kinases, mostly incomplete unproductive complexes are formed. In fact, one of the scaffolds of the JNK pathway, JIP1, was first discovered as a suppressor of JNK signaling upon its overexpression.[98] Arr3 activates the JNK pathway by acting as a scaffold.[42,69,70] Therefore, our finding that low and high Arr3 expression levels have opposite effects on the behavioral sensitization, with a low Arr3 level promoting and a high level inhibiting sensitization in both behavioral paradigms, is not surprising. The most parsimonious explanation is that Arr3 acts as a scaffold for the JNK pathway in striatal neurons *in vivo* as in cultured cells. Our data explain the previously published result that AAV-mediated overexpression of Arr3 in the lesioned striatum of WT hemiparkinsonian rodents suppressed AIMs.[67] Although no quantification of the Arr3 expression levels was provided in that study,[67] it is well known that AAVs usually yield high expression. The LV-mediated expression is in the range of 25%–30% of the endogenous Arr3 level, whereas the AAV-mediated Arr3 expression exceeded the endogenous level ~10-fold. Thus, our data provide the first experimental evidence of the Arr3 scaffolding action for the JNK activation cascade in living animals.

Unilaterally 6-OHDA-lesioned rodents have been extensively used as an animal model of LID in PD.[23,99,100] We employed it as a model of drug-induced long-term adaptations manifesting themselves at the behavioral level, focusing on the underlying signaling mechanisms. Such adaptations are not unique for LID and/or PD but are induced by other dopaminergic and non-dopaminergic drugs, although the signaling mechanisms involved in each case might differ. Signaling plasticity could cause detrimental side effects limiting the therapeutic utility of drugs (e.g., in case of LID), or contribute to their addictive properties. Understanding of the molecular mechanisms involved is necessary for the development of new or improvement of existing therapies. The ability of the short Arr3-derived T1A peptide to substitute for the full-length Arr3 *in vivo* suggests that peptide-based tools can be developed. We envision Arr3-derived peptides that inhibit JNK3 activity via a dominant-negative action. Such peptides delivered at high levels would act similarly to a high concentration of full-length Arr3. Alternatively, peptides that bind only one or two kinases of the pathway, recruiting them away from productive scaffolds, would also act as dominant-negative inhibitors. Such peptides could be used to control Arr3-dependent regulation of the JNK pathway for therapeutic purposes in human patients with a normal complement of WT Arr3.

Limitations of the study

There are two major limitations.

(1) It is assumed that chronic dopaminergic stimulation initiates signaling adaptations eventually leading to behavioral sensitization, with the Arr3-dependent JNK3 activation being the key intermediate mechanism. However, the molecular mechanism linking stimulation of DA receptors upon L-DOPA treatment with the activation of JNK3 remains to be elucidated.

(2) While the c-Jun phosphorylation correlates with the sensitization deficit seen in A3KO mice and the behavioral rescue, the exact substrate phosphorylation of which by JNK3 is necessary for behavioral sensitization also remains unknown.

STAR★METHODS

Detailed methods are provided in the online version of this paper and include the following:

- KEY RESOURCES TABLE
- RESOURCE AVAILABILITY
  - Lead contact
  - Materials availability
  - Data and code availability
- EXPERIMENTAL MODEL AND STUDY PARTICIPANT DETAILS
  - Cell lines
  - Animals
- METHOD DETAILS
  - Virus construction and preparation
  - Animal surgeries and virus injection
  - Animal behavior
  - Cylinder test
  - Tissue preparation
  - Western blot
  - Immunohistochemistry
  - In-cell JNK phosphorylation assay
  - Immunoprecipitation from the striatal tissue
- QUANTIFICATION AND STATISTICAL ANALYSIS

SUPPLEMENTAL INFORMATION

Supplemental information can be found online at https://doi.org/10.1016/j.xcrm.2024.101623.

ACKNOWLEDGMENTS

We thank Dr. Robert J. Lefkowitz (Duke University) for the gift of the arrestin knockout mice. We are grateful to Dr. John F. Neumaier (University of Washington) for the gift of the rat enkephalin and dynorphin promoter vectors. This work was supported by NIH grants RO1 NS065868 and R21 DA030103 (to E.V.G.) and R35 GM122491 (to V.V.G.).

AUTHOR CONTRIBUTIONS

M.R.A., C.Z., J.L.D., M.S.A., C.G., F.S.P., and E.V.G. conducted the study. M.R.A., E.V.G., and V.V.G. designed the experiments. E.V.G. and V.V.G. wrote the paper.

DECLARATION OF INTERESTS

E.V.G. and V.V.G. have a patent related to this work: "Peptide Regulators Of JNK Family Kinases". Patent no.: US 10,369,187 B2, date of patent: Aug. 6, 2019.

Received: November 8, 2023
Revised: April 15, 2024
Accepted: June 5, 2024
Published: June 26, 2024

REFERENCES

1. Gurevich, V.V., and Gurevich, E.V. (2006). The structural basis of arrestin-mediated regulation of G protein-coupled receptors. Pharmacol. Ther. *110*, 465–502.

2. Gurevich, V.V., and Gurevich, E.V. (2019). GPCR Signaling Regulation: The Role of GRKs and Arrestins. Front. Pharmacol. *10*, 125. https://doi.org/10.3389/fphar.2019.00125.

3. Gurevich, V.V., and Gurevich, E.V. (2023). Mechanisms of Arrestin-Mediated Signaling. Curr. Protoc. *3*, e821. https://doi.org/10.1002/cpz1.821.

4. Wess, J., Oteng, A.B., Rivera-Gonzalez, O., Gurevich, E.V., and Gurevich, V.V. (2023). β-Arrestins: Structure, Function, Physiology, and Pharmacological Perspectives. Pharmacol. Rev. *75*, 854–884. https://doi.org/10.1124/pharmrev.121.000302.

5. Peterson, Y.K., and Luttrell, L.M. (2017). The Diverse Roles of Arrestin Scaffolds in G Protein-Coupled Receptor Signaling. Pharmacol. Rev. *69*, 256–297.

6. Bohn, L.M., Gainetdinov, R.R., Sotnikova, T.D., Medvedev, I.O., Lefkowitz, R.J., Dykstra, L.A., and Caron, M.G. (2003). Enhanced rewarding properties of morphine, but not cocaine, in beta(arrestin)-2 knock-out mice. J. Neurosci. *23*, 10265–10273.

7. Bohn, L.M., Lefkowitz, R.J., Gainetdinov, R.R., Peppel, K., Caron, M.G., and Lin, F.T. (1999). Enhanced morphine analgesia in mice lacking beta-arrestin2. Science *286*, 2495–2498.

8. Gainetdinov, R.R., Bohn, L.M., Walker, J.K., Laporte, S.A., Macrae, A.D., Caron, M.G., Lefkowitz, R.J., and Premont, R.T. (1999). Muscarinic supersensitivity and impaired receptor desensitization in G protein-coupled receptor kinase 5-deficient mice. Neuron *24*, 1029–1036.

9. Beaulieu, J.M., Sotnikova, T.D., Marion, S., Lefkowitz, R.J., Gainetdinov, R.R., and Caron, M.G. (2005). An Akt/beta-arrestin 2/PP2A signaling complex mediates dopaminergic neurotransmission and behavior. Cell *122*, 261–273.

10. Zurkovsky, L., Sedaghat, K., Ahmed, M.R., Gurevich, V.V., and Gurevich, E.V. (2017). Arrestin-2 and arrestin-3 differentially modulate locomotor responses and sensitization to amphetamine. Neuropharmacology *121*, 20–29. https://doi.org/10.1016/j.neuropharm.2017.04.021.

11. Urs, N.M., Gee, S.M., Pack, T.F., McCorvy, J.D., Evron, T., Snyder, J.C., Yang, X., Rodriguiz, R.M., Borrelli, E., Wetsel, W.C., et al. (2016). Distinct cortical and striatal actions of a β-arrestin-biased dopamine D2 receptor ligand reveal unique antipsychotic-like properties. Proc. Natl. Acad. Sci. USA *113*, E8178–E8186.

12. Li, M. (2016). Antipsychotic-induced sensitization and tolerance: Behavioral characteristics, developmental impacts, and neurobiological mechanisms. J. Psychopharmacol. *30*, 749–770. https://doi.org/10.1177/0269881116654697.

13. Qiao, J., Li, H., and Li, M. (2013). Olanzapine Sensitization and Clozapine Tolerance: From Adolescence to Adulthood in the Conditioned Avoidance Response Model. Neuropsychopharmacology *38*, 513–524. https://doi.org/10.1038/npp.2012.213.

14. Colvin, L.A., Bull, F., and Hales, T.G. (2019). Perioperative opioid analgesia—when is enough too much? A review of opioid-induced tolerance and hyperalgesia. Lancet *393*, 1558–1568. https://doi.org/10.1016/S0140-6736(19)30430-1.

15. Cenci, M.A. (2007). Dopamine dysregulation of movement control in L-DOPA-induced dyskinesia. Trends Neurosci. *30*, 236–243.

16. Sgambato-Faure, V., Buggia, V., Gilbert, F., Lévesque, D., Benabid, A.L., and Berger, F. (2005). Coordinated and spatial upregulation of arc in striatonigral neurons correlates with L-dopa-induced behavioral sensitization in dyskinetic rats. J. Neuropathol. Exp. Neurol. *64*, 936–947.

17. Li, L., Homan, K.T., Vishnivetskiy, S.A., Manglik, A., Tesmer, J.J.G., Gurevich, V.V., and Gurevich, E.V. (2015). G Protein-coupled Receptor Kinases of the GRK4 Protein Subfamily Phosphorylate Inactive G Protein-coupled Receptors (GPCRs). J. Biol. Chem. *290*, 10775–10790.

18. Kim, K.M., Valenzano, K.J., Robinson, S.R., Yao, W.D., Barak, L.S., and Caron, M.G. (2001). Differential regulation of the dopamine D2 and D3 receptors by G protein-coupled receptor kinases and beta-arrestins. J. Biol. Chem. *276*, 37409–37414. https://doi.org/10.1074/jbc.M106728200.

19. Kim, K.M. (2023). Unveiling the Differences in Signaling and Regulatory Mechanisms between Dopamine D(2) and D(3) Receptors and Their Impact on Behavioral Sensitization. Int. J. Mol. Sci. *24*, 6742. https://doi.org/10.3390/ijms24076742.

20. Burström, V., Ågren, R., Betari, N., Valle-León, M., Garro-Martínez, E., Ciruela, F., and Sahlholm, K. (2023). Dopamine-induced arrestin recruitment and desensitization of the dopamine D4 receptor is regulated by G protein-coupled receptor kinase-2. Front. Pharmacol. *14*, 1087171. https://doi.org/10.3389/fphar.2023.1087171.

21. Yang, Y., Lewis, M.M., Huang, X., Dokholyan, N.V., and Mailman, R.B. (2022). Dopamine D(1) receptor-mediated β-arrestin signaling: Insight from pharmacology, biology, behavior, and neurophysiology. Int. J. Biochem. Cell Biol. *148*, 106235. https://doi.org/10.1016/j.biocel.2022.106235.

22. Moritz, A.E., Madaras, N.S., Rankin, M.L., Inbody, L.R., and Sibley, D.R. (2023). Delineation of G Protein-Coupled Receptor Kinase Phosphorylation Sites within the D(1) Dopamine Receptor and Their Roles in Modulating β-Arrestin Binding and Activation. Int. J. Mol. Sci. *24*, 6599. https://doi.org/10.3390/ijms24076599.

23. Bastide, M.F., Meissner, W.G., Picconi, B., Fasano, S., Fernagut, P.O., Feyder, M., Francardo, V., Alcacer, C., Ding, Y., Brambilla, R., et al. (2015). Pathophysiology of L-dopa-induced motor and non-motor complications in Parkinson's disease. Prog. Neurobiol. *132*, 96–168.

24. Delage, C., Morel, A., de Witt, P., Jauffret-Roustide, M., Bloch, V., Noble, F., Vorspan, F., and Marie, N. (2023). Behavioral sensitization to psychostimulants and opioids: What is known in rodents and what still needs to be explored in humans? Prog. Neuro-Psychopharmacol. Biol. Psychiatry *127*, 110824. https://doi.org/10.1016/j.pnpbp.2023.110824.

25. Jeffery, D.S., and Peter, W.K. (2011). Drug Wanting: Behavioral Sensitization and Relapse to Drug-Seeking Behavior. Pharmacol. Rev. *63*, 348. https://doi.org/10.1124/pr.109.001933.

26. Abe, Y., Yagishita, S., Sano, H., Sugiura, Y., Dantsuji, M., Suzuki, T., Mochizuki, A., Yoshimaru, D., Hata, J., Matsumoto, M., et al. (2023). Shared GABA transmission pathology in dopamine agonist- and antagonist-induced dyskinesia. Cell Rep. Med. *4*, 101208. https://doi.org/10.1016/j.xcrm.2023.101208.

27. Morin, N., Jourdain, V.A., and Di Paolo, T. (2014). Modeling dyskinesia in animal models of Parkinson disease. Exp. Neurol. *256*, 105–116. https://doi.org/10.1016/j.expneurol.2013.01.024.

28. Cenci, M.A., and Lundblad, M. (2007). Ratings of L-DOPA-induced dyskinesia in the unilateral 6-OHDA lesion model of Parkinson's disease in rats and mice. Curr. Protoc. Neurosci. *9*.

29. Francardo, V., and Cenci, M.A. (2014). Investigating the molecular mechanisms of L-DOPA-induced dyskinesia in the mouse. Parkinsonism Relat. Disorders *20*, S20–S22. https://doi.org/10.1016/s1353-8020(13)70008-7.

30. Francardo, V., Recchia, A., Popovic, N., Andersson, D., Nissbrandt, H., and Cenci, M.A. (2011). Impact of the lesion procedure on the profiles of motor impairment and molecular responsiveness to L-DOPA in the 6-hydroxydopamine mouse model of Parkinson's disease. Neurobiol. Dis. *42*, 327–340. https://doi.org/10.1016/j.nbd.2011.01.024.

31. Alcacer, C., Santini, E., Valjent, E., Gaven, F., Girault, J.A., and Hervé, D. (2012). Gα(olf) mutation allows parsing the role of cAMP-dependent and extracellular signal-regulated kinase-dependent signaling in L-3,4-dihydroxyphenylalanine-induced dyskinesia. J. Neurosci. *32*, 5900–5910. https://doi.org/10.1523/jneurosci.0837-12.2012.

32. Bychkov, E., Ahmed, M.R.,, Dalby, K.N., and Gurevich, E.V. (2007). Dopamine depletion and subsequent treatment with L-DOPA, but not the long-lived dopamine agonist pergolide, enhances activity of the Akt pathway in the rat striatum. J. Neurochem. *102*, 699–711.

33. Pavón, N., Martín, A.B., Mendialdua, A., and Moratalla, R. (2006). ERK phosphorylation and FosB expression are associated with L-DOPA-induced dyskinesia in hemiparkinsonian mice. Biol. Psychiatr. *59*, 64–74. https://doi.org/10.1016/j.biopsych.2005.05.044.

34. Ahmed, M.R., Bychkov, E., Gurevich, V.V., Benovic, J.L., and Gurevich, E.V. (2007). Altered expression and subcellular distribution of GRK subtypes in the dopamine-depleted rat basal ganglia is not normalized by L-DOPA treatment. J. Neurochem. *104*, 1622–1636.

35. Ahmed, M.R., Berthet, A., Bychkov, E., Porras, G., Li, Q., Bioulac, B.H., Carl, Y.T., Bloch, B., Kook, S., Aubert, I., et al. (2010). Lentiviral overexpression of GRK6 alleviates L-dopa-induced dyskinesia in experimental Parkinson's disease. Sci. Transl. Med. *2*, 28ra28.

36. Gurevich, V.V., and Gurevich, E.V. (2014). Overview of different mechanisms of arrestin-mediated signaling. Curr. Protoc. Pharmacol. *67*, 10.2.10.1–2.10.9. https://doi.org/10.1002/0471141755.ph0210s67.

37. Gurevich, V.V., and Gurevich, E.V. (2018). Arrestins and G proteins in cellular signaling: The coin has two sides. Sci. Signal. *11*, eaav1646.

38. Gurevich, V.V., and Gurevich, E.V. (2015). Analyzing the roles of multifunctional proteins in cells: The case of arrestins and GRKs. Crit. Rev. Biochem. Mol. Biol. *50*, 440–452.

39. McDonald, P.H., Chow, C.W., Miller, W.E., Laporte, S.A., Field, M.E., Lin, F.T., Davis, R.J., and Lefkowitz, R.J. (2000). Beta-arrestin 2: a receptor-regulated MAPK scaffold for the activation of JNK3. Science *290*, 1574–1577.

40. Seo, J., Tsakem, E.L., Breitman, M., and Gurevich, V.V. (2011). Identification of arrestin-3-specific residues necessary for JNK3 kinase activation. J. Biol. Chem. *286*, 27894–27901.

41. Song, X., Coffa, S., Fu, H., and Gurevich, V.V. (2009). How does arrestin assemble MAPKs into a signaling complex? J. Biol. Chem. *284*, 685–695.

42. Kook, S., Zhan, X., Kaoud, T.S., Dalby, K.N., Gurevich, V.V., and Gurevich, E.V. (2014). Arrestin-3 binds JNK1 and JNK2 and facilitates the activation of these ubiquitous JNK isoforms in cells via scaffolding. J. Biol. Chem. *288*, 37332–37342.

43. Zhan, X., Kook, S., Gurevich, E.V., and Gurevich, V.V. (2014). Arrestin-Dependent Activation of JNK Family Kinases. In Arrestins - Pharmacology and Therapeutic Potential, V.V. Gurevich, ed. (Springer Berlin Heidelberg), pp. 259–280. https://doi.org/10.1007/978-3-642-41199-1_13.

44. Zhan, X., Kaoud, T.S., Dalby, K.N., Gurevich, E.V., and Gurevich, V.V. (2023). Arrestin-3-Dependent Activation of c-Jun N-Terminal Kinases (JNKs). Curr. Protoc. *3*, e839. https://doi.org/10.1002/cpz1.839.

45. Zhan, X., Stoy, H., Kaoud, T.S., Perry, N.A., Chen, Q., Perez, A., Els-Heindl, S., Slagis, J.V., Iverson, T.M., Beck-Sickinger, A.G., et al. (2016). Peptide mini-scaffold facilitates JNK3 activation in cells. Sci. Rep. *6*, 21025.

46. Perry-Hauser, N.A., Kaoud, T.S., Stoy, H., Zhan, X., Chen, Q., Dalby, K.N., Iverson, T.M., Gurevich, V.V., and Gurevich, E.V. (2022). Short Arrestin-3-Derived Peptides Activate JNK3 in Cells. Int. J. Mol. Sci. *23*, 8679. https://doi.org/10.3390/ijms23158679.

47. Gerfen, C.R. (2022). Segregation of D1 and D2 dopamine receptors in the striatal direct and indirect pathways: An historical perspective. Front. Synaptic Neurosci. *14*, 1002960. https://doi.org/10.3389/fnsyn.2022.1002960.

48. Keeler, J.F., Pretsell, D.O., and Robbins, T.W. (2014). Functional implications of dopamine D1 vs. D2 receptors: A 'prepare and select' model of the striatal direct vs. indirect pathways. Neuroscience *282*, 156–175. https://doi.org/10.1016/j.neuroscience.2014.07.021.

49. Bychkov, E., Zurkovsky, L., Garret, M.B., Ahmed, M.R., and Gurevich, E.V. (2012). Distinct Cellular and Subcellular Distributions of G Protein-Coupled Receptor Kinase and Arrestin Isoforms in the Striatum. PLoS One *7*, e48912. https://doi.org/10.1371/journal.pone.0048912.

50. Ferguson, S.M., Eskenazi, D., Ishikawa, M., Wanat, M.J., Phillips, P.E.M., Dong, Y., Roth, B.L., and Neumaier, J.F. (2011). Transient neuronal inhibition reveals opposing roles of indirect and direct pathways in sensitization. Nat. Neurosci. *14*, 22–24.

51. Bochkov, Y.A., and Palmenberg, A.C. (2006). Translational efficiency of EMCV IRES in bicistronic vectors is dependent upon IRES sequence and gene location. Biotechniques *41*, 283–290.

52. Hoover, B.R., and Marshall, J.F. (2002). Further characterization of preproenkephalin mRNA-containing cells in the rodent globus pallidus. Neuroscience *111*, 111–125. https://doi.org/10.1016/s0306-4522(01)00565-6.

53. Medina, L., Abellán, A., Vicario, A., and Desfilis, E. (2014). Evolutionary and developmental contributions for understanding the organization of the basal ganglia. Brain Behav. Evol. *83*, 112–125. https://doi.org/10.1159/000357832.

54. Fallon, J.H., and Leslie, F.M. (1986). Distribution of dynorphin and enkephalin peptides in the rat brain. J. Comp. Neurol. *249*, 293–336. https://doi.org/10.1002/cne.902490302.

55. Yang, F.C., Vivian, J.L., Traxler, C., Shapiro, S.M., and Stanford, J.A. (2022). MGE-Like Neural Progenitor Cell Survival and Expression of Parvalbumin and Proenkephalin in a Jaundiced Rat Model of Kernicterus. Cell Transplant. *31*, 9636897221101116. https://doi.org/10.1177/09636897221101116.

56. Ahmed, M.R., Bychkov, E., Kook, S., Zurkovsky, L., Dalby, K.N., and Gurevich, E.V. (2015). Overexpression of GRK6 rescues L-DOPA-induced signaling abnormalities in the dopamine-depleted striatum of hemiparkinsonian rats. Exp. Neurol. *266*, 42–54.

57. Johnson, G.L., Dohlman, H.G., and Graves, L.M. (2005). MAPK kinase kinases (MKKKs) as a target class for small-molecule inhibition to modulate signaling networks and gene expression. Curr. Opin. Chem. Biol. *9*, 325–331. https://doi.org/10.1016/j.cbpa.2005.04.004.

58. Johnson, G.L. (2011). Defining MAPK interactomes. ACS Chem. Biol. *6*, 18–20.

59. Cuevas, B.D., Abell, A.N., and Johnson, G.L. (2007). Role of mitogen-activated protein kinase kinase kinases in signal integration. Oncogene *26*, 3159–3171. https://doi.org/10.1038/sj.onc.1210409.

60. Gallo, K.A., and Johnson, G.L. (2002). Mixed-lineage kinase control of JNK and p38 MAPK pathways. Nat. Rev. Mol. Cell Biol. *3*, 663–672. https://doi.org/10.1038/nrm906.

61. Köster, K.A., Dethlefs, M., Duque Escobar, J., and Oetjen, E. (2024). Regulation of the Activity of the Dual Leucine Zipper Kinase by Distinct Mechanisms. Cells *13*, 333. https://doi.org/10.3390/cells13040333.

62. Luttrell, L.M., Roudabush, F.L., Choy, E.W., Miller, W.E., Field, M.E., Pierce, K.L., and Lefkowitz, R.J. (2001). Activation and targeting of extracellular signal-regulated kinases by beta-arrestin scaffolds. Proc. Natl. Acad. Sci. USA *98*, 2449–2454.

63. Ono, K., and Han, J. (2000). The p38 signal transduction pathway: activation and function. Cell. Signal. *12*, 1–13. https://doi.org/10.1016/s0898-6568(99)00071-6.

64. Coffey, E.T. (2014). Nuclear and cytosolic JNK signalling in neurons. Nat. Rev. Neurosci. *15*, 285–299. https://doi.org/10.1038/nrn3729.

65. Bogoyevitch, M.A., and Kobe, B. (2006). Uses for JNK: the Many and Varied Substrates of the c-Jun N-Terminal Kinases. Microbiol. Mol. Biol. Rev. *70*, 1061–1095.

66. Hollos, P., Marchisella, F., and Coffey, E.T. (2018). JNK Regulation of Depression and Anxiety. Brain Plast. *3*, 145–155. https://doi.org/10.3233/bpl-170062.

67. Urs, N.M., Bido, S., Peterson, S.M., Daigle, T.L., Bass, C.E., Gainetdinov, R.R., Bezard, E., and Caron, M.G. (2015). Targeting β-arrestin2 in the treatment of L-DOPA-induced dyskinesia in Parkinson's disease. Proc. Natl. Acad. Sci. USA *112*, E2517–E2526.

68. Weston, C.R., and Davis, R.J. (2007). The JNK signal transduction pathway. Curr. Opin. Cell Biol. *19*, 142–149. https://doi.org/10.1016/j.ceb.2007.02.001.

69. Zhan, X., Kaoud, T.S., Kook, S., Dalby, K.N., and Gurevich, V.V. (2013). JNK3 enzyme binding to arrestin-3 differentially affects the recruitment of upstream mitogen-activated protein (MAP) kinase kinases. J. Biol. Chem. *288*, 28535–28547.

70. Zhan, X., Kaoud, T.S., Dalby, K.N., and Gurevich, V.V. (2011). Nonvisual arrestins function as simple scaffolds assembling the MKK4-JNK3α2 signaling complex. Biochemistry *50*, 10520–10529.

71. Levchenko, A., Bruck, J., and Sternberg, P.W. (2000). Scaffold proteins may biphasically affect the levels of mitogen-activated protein kinase signaling and reduce its threshold properties. Proc. Natl. Acad. Sci. USA *97*, 5818–5823.

72. Ahmed, M.R., Bychkov, E., Li, L., Gurevich, V.V., and Gurevich, E.V. (2015). GRK3 suppresses L-DOPA-induced dyskinesia in the rat model of Parkinson's disease via its RGS homology domain. Sci. Rep. *5*, 10920.

73. Andreoli, L., Abbaszadeh, M., Cao, X., and Cenci, M.A. (2021). Distinct patterns of dyskinetic and dystonic features following D1 or D2 receptor stimulation in a mouse model of parkinsonism. Neurobiol. Dis. *157*, 105429. https://doi.org/10.1016/j.nbd.2021.105429.

74. Song, X., Vishnivetskiy, S.A., Seo, J., Chen, J., Gurevich, E.V., and Gurevich, V.V. (2011). Arrestin-1 expression level in rods: balancing functional performance and photoreceptor health. Neuroscience *174*, 37–49.

75. Gurevich, V.V., and Gurevich, E.V. (2014). Extensive shape shifting underlies functional versatility of arrestins. Curr. Opin. Cell Biol. *27*, 1–9.

76. Gurevich, V.V., and Gurevich, E.V. (2019). Plethora of functions packed into 45 kDa arrestins: biological implications and possible therapeutic strategies. Cell. Mol. Life Sci. *76*, 4413–4421.

77. Xiao, K., McClatchy, D.B., Shukla, A.K., Zhao, Y., Chen, M., Shenoy, S.K., Yates, J.R., and Lefkowitz, R.J. (2007). Functional specialization of beta-arrestin interactions revealed by proteomic analysis. Proc. Natl. Acad. Sci. USA *104*, 12011–12016.

78. Urs, N.M., Daigle, T.L., and Caron, M.G. (2011). A dopamine D1 receptor-dependent β-arrestin signaling complex potentially regulates morphine-induced psychomotor activation but not reward in mice. Neuropsychopharmacology *36*, 551–558. https://doi.org/10.1038/npp.2010.186.

79. Busquets, O., Ettcheto, M., Cano, A., R Manzine, P., Sánchez-Lopez, E., Espinosa-Jiménez, T., Verdaguer, E., Dario Castro-Torres, R., Beas-Zarate, C., X Sureda, F., et al. (2019). Role of c-Jun N-Terminal Kinases (JNKs) in Epilepsy and Metabolic Cognitive Impairment. Int. J. Mol. Sci. *21*, 255. https://doi.org/10.3390/ijms21010255.

80. Musi, C.A., Agrò, G., Santarella, F., Iervasi, E., and Borsello, T. (2020). JNK3 as Therapeutic Target and Biomarker in Neurodegenerative and Neurodevelopmental Brain Diseases. Cells *9*, 2190. https://doi.org/10.3390/cells9102190.

81. Hepp Rehfeldt, S.C., Majolo, F., Goettert, M.I., and Laufer, S. (2020). c-Jun N-Terminal Kinase Inhibitors as Potential Leads for New Therapeutics for Alzheimer's Diseases. Int. J. Mol. Sci. *21*, 9677. https://doi.org/10.3390/ijms21249677.

82. Nakano, R., Nakayama, T., and Sugiya, H. (2020). Biological Properties of JNK3 and Its Function in Neurons, Astrocytes, Pancreatic β-Cells and Cardiovascular Cells. Cells *9*, 1802. https://doi.org/10.3390/cells9081802.

83. Priori, E.C., Musi, C.A., Giani, A., Colnaghi, L., Milic, I., Devitt, A., Borsello, T., and Repici, M. (2023). JNK Activation Correlates with Cognitive Impairment and Alteration of the Post-Synaptic Element in the 5xFAD AD Mouse Model. Cells *12*, 904. https://doi.org/10.3390/cells12060904.

84. Anfinogenova, N.D., Quinn, M.T., Schepetkin, I.A., and Atochin, D.N. (2020). Alarmins and c-Jun N-Terminal Kinase (JNK) Signaling in Neuroinflammation. Cells *9*, 2350. https://doi.org/10.3390/cells9112350.

85. de Los Reyes Corrales, T., Losada-Pérez, M., and Casas-Tintó, S. (2021). JNK Pathway in CNS Pathologies. Int. J. Mol. Sci. *22*, 3883. https://doi.org/10.3390/ijms22083883.

86. Aubert, I., Bezard, E., Guigoni, C., Håkansson, K., Li, Q., Dovero, S., Barthe, N., Bioulac, B.H., Gross, C.E., Fisone, G., and Bloch, B. (2005). Increased D1 dopamine receptor signaling in levodopa-induced dyskinesia. Ann. Neurol. *57*, 17–26.

87. Gerfen, C.R. (2000). Dopamine-mediated gene regulation in models of Parkinson's disease. Ann. Neurol. *47*, S42–S52.

88. Gerfen, C.R., Miyachi, S., Paletzki, R., and Brown, P. (2002). D1 dopamine receptor supersensitivity in the dopamine-depleted striatum results from a switch in the regulation of ERK1/2/MAP kinase. J. Neurosci. *22*, 5042–5054.

89. Lefkowitz, R.J., and Whalen, E.J. (2004). beta-arrestins: traffic cops of cell signaling. Curr. Opin. Cell Biol. *16*, 162–168. https://doi.org/10.1016/j.ceb.2004.01.001.

90. Lefkowitz, R.J., and Shenoy, S.K. (2005). Transduction of receptor signals by beta-arrestins. Science *308*, 512–517.

91. Breitman, M., Kook, S., Gimenez, L.E., Lizama, B.N., Palazzo, M.C., Gurevich, E.V., and Gurevich, V.V. (2012). Silent scaffolds: inhibition OF c-Jun N-terminal kinase 3 activity in cell by dominant-negative arrestin-3 mutant. J. Biol. Chem. *287*, 19653–19664.

92. Miller, W.E., McDonald, P.H., Cai, S.F., Field, M.E., Davis, R.J., and Lefkowitz, R.J. (2001). Identification of a motif in the carboxyl terminus of beta -arrestin2 responsible for activation of JNK3. J. Biol. Chem. *276*, 27770–27777.

93. Zheng, C., Weinstein, L.D., Nguyen, K.K., Grewal, A., Gurevich, E.V., and Gurevich, V.V. (2023). GPCR Binding and JNK3 Activation by Arrestin-3 Have Different Structural Requirements. Cells *12*, 1563. https://doi.org/10.3390/cells12121563.

94. Gurevich, V.V., and Gurevich, E.V. (2018). Arrestin-mediated signaling: Is there a controversy? World J. Biol. Chem. *9*, 25–35. https://doi.org/10.4331/wjbc.v9.i3.25.

95. Hao, Y., Frey, E., Yoon, C., Wong, H., Nestorovski, D., Holzman, L.B., Giger, R.J., DiAntonio, A., and Collins, C. (2016). An evolutionarily conserved mechanism for cAMP elicited axonal regeneration involves direct activation of the dual leucine zipper kinase DLK. Elife *5*, e14048. https://doi.org/10.7554/eLife.14048.

96. Ghosh-Roy, A., Wu, Z., Goncharov, A., Jin, Y., and Chisholm, A.D. (2010). Calcium and cyclic AMP promote axonal regeneration in Caenorhabditis elegans and require DLK-1 kinase. J. Neurosci. *30*, 3175–3183. https://doi.org/10.1523/jneurosci.5464-09.2010.

97. Levchenko, A., Bruck, J., and Sternberg, P.W. (2004). Regulatory modules that generate biphasic signal response in biological systems. Off. Syst. *1*, 139–148.

98. Dickens, M., Rogers, J.S., Cavanagh, J., Raitano, A., Xia, Z., Halpern, J.R., Greenberg, M.E., Sawyers, C.L., and Davis, R.J. (1997). A Cytoplasmic Inhibitor of the JNK Signal Transduction Pathway. Science *277*, 693–696. https://doi.org/10.1126/science.277.5326.693.

99. Chen, X., Wang, Y., Wu, H., Cheng, C., and Le, W. (2020). Research advances on L-DOPA-induced dyskinesia: from animal models to human disease. Neurol. Sci. *41*, 2055–2065. https://doi.org/10.1007/s10072-020-04333-5.

100. Cenci, M.A., and Björklund, A. (2020). Animal models for preclinical Parkinson's research: An update and critical appraisal. Prog. Brain Res. *252*, 27–59. https://doi.org/10.1016/bs.pbr.2020.02.003.

101. Vishnivetskiy, S.A., Zhan, X., and Gurevich, V.V. (2023). Expression of Untagged Arrestins in E. coli and Their Purification. Curr. Protoc. *3*, e832. https://doi.org/10.1002/cpz1.832.

102. Boix, J., Padel, T., and Paul, G. (2015). A partial lesion model of Parkinson's disease in mice – Characterization of a 6-OHDA-induced medial forebrain bundle lesion. Behav. Brain Res. *284*, 196–206. https://doi.org/10.1016/j.bbr.2015.01.053.

103. Mendes-Pinheiro, B., Soares-Cunha, C., Marote, A., Loureiro-Campos, E., Campos, J., Barata-Antunes, S., Monteiro-Fernandes, D., Santos, D., Duarte-Silva, S., Pinto, L., and José Salgado, A. (2021). Unilateral Intrastriatal 6-Hydroxydopamine Lesion in Mice: A Closer Look into

Non-Motor Phenotype and Glial Response. Int. J. Mol. Sci. *22*, 11530. https://doi.org/10.3390/ijms222111530.

104. Lundblad, M., Andersson, M., Winkler, C., Kirik, D., Wierup, N., and Cenci, M.A. (2002). Pharmacological validation of behavioural measures of akinesia and dyskinesia in a rat model of Parkinson's disease. Eur. J. Neurosci. *15*, 120–132.

105. Lee, C.S., Cenci, M.A., Schulzer, M., and Björklund, A. (2000). Embryonic ventral mesencephalic grafts improve levodopa-induced dyskinesia in a rat model of Parkinson's disease. Brain *123*, 1365–1379.

106. Mela, F., Marti, M., Dekundy, A., Danysz, W., Morari, M., and Cenci, M.A. (2007). Antagonism of metabotropic glutamate receptor type 5 attenuates l-DOPA-induced dyskinesia and its molecular and neurochemical correlates in a rat model of Parkinson's disease. J. Neurochem. *101*, 483–497.

107. Tamura, S., Morikawa, Y., Iwanishi, H., Hisaoka, T., and Senba, E. (2004). Foxp1 gene expression in projection neurons of the mouse striatum. Neuroscience *124*, 261–267.

108. Zhan, X., Kook, S., Kaoud, T.S., Dalby, K.N., Gurevich, E.V., and Gurevich, V.V. (2015). Arrestin-3-Dependent Activation of c-Jun N-Terminal Kinases (JNKs). Curr. Protoc. Pharmacol. *68*, 2.12.1–2.12.26. https://doi.org/10.1002/0471141755.ph0212s68.

109. Chen, Q., Perry, N.A., Vishnivetskiy, S.A., Berndt, S., Gilbert, N.C., Zhuo, Y., Singh, P.K., Tholen, J., Ohi, M.D., Gurevich, E.V., et al. (2017). Structural basis of arrestin-3 activation and signaling. Nat. Commun. *8*, 1427. https://doi.org/10.1038/s41467-017-01218-8.

110. Ahmed, M.R., Zhan, X., Song, X., Kook, S., Gurevich, V.V., and Gurevich, E.V. (2011). Ubiquitin ligase parkin promotes Mdm2-arrestin interaction but inhibits arrestin ubiquitination. Biochemistry *50*, 3749–3763.

STAR★METHODS

KEY RESOURCES TABLE

REAGENT or RESOURCE	SOURCE	IDENTIFIER
Antibodies		
Rabbit polyclonal anti-arrestin-3 antibody	Ahmed, Bychkov et al. 2007[34]	N/A
Mouse monoclonal anti-GFP antibody	Takara (Clontech)	Cat# JL-8, RRID: AB_10013427
Chicken polyclonal anti-GFP antibody	Invitrogen	Cat#: A10262 RRID: AB_2534023
Mouse monoclonal HIV1p24 antibody	ThermoFisher	Cat# MA1-71521 RRID: AB_962115
Rabbit anti-tyrosine hydroxylase (TH) antibody	Chemicon	Cat# AB152 RRID: AB_390204
Sheep anti-TH antibody	Novex	Cat# NB300-110 RRID: AB_10002491
Rabbit anti-FOXP1 antibody	Cell Signaling Technologies	Cat#2005 RRID: AB_2106979
Rabbit monoclonal anti-HA antibody	Cell Signaling Technologies	Cat# 3724 RRID: AB_1549585
Anti-phospho JNK (pThr183/pTyr185) antibody	Cell Signaling Technologies	Cat# 4668 RRID: AB_823588
Anti-phospho JNK (pThr183/pTyr185) antibody	Cell Signaling Technologies	Cat# 9251 RRID: AB_331659
Rabbit anti-SAPK/JNK antibody	Cell Signaling Technologies	Cat#9152 RRID: AB_330905
Rabbit JNK3-specific antibody	Cell Signaling Technologies	Cat#2305 RRID: AB_2281744
Mouse JNK3-specific antibody	Santa Cruz Biotechnology	Cat# sc-130075 RRID: AB_2141575
Rabbit anti-phospho-cJun (pSer73) antibody	Cell Signaling Technologies	Cat#3270 RRID: AB_2895041
Mouse monoclonal anti-cJun antibody	Cell Signaling Technologies	Cat#2315 RRID: AB_490780
Mouse monoclonal anti-phospho-ERK1/2 (pThr202/pTyr204)	Cell Signaling Technologies	Cat#9106 RRID: AB_331768
Rabbit anti-ERK1/2 antibody	Cell Signaling Technologies	Cat#9102 RRID: AB_330744
Rabbit anti-phospho-Akt (pT308) antibody	Cell Signaling Technologies	Cat#9275 RRID: AB_329828
Rabbit anti-phospho-Akt (pS473) antibody	Cell Signaling Technologies	Cat#4060 RRID: AB_2315049
Rabbit anti-Akt antibody	Cell Signaling Technologies	Cat#9272 RRID: AB_329827
Rabbit monoclonal anti-phospho-p38 antobody	Cell Signaling Technologies	Cat#4511 RRID: AB_2139682
Rabbit anti p38 antibody	Cell Signaling Technologies	Cat#9212 RRID: AB_330713
Goat anti-rabbit horseradish peroxidase-conjugated (H+L) secondary antibody	Jackson ImmunoResearch Laboratories	Cat# 111-035-144 RRID: AB_2307391
Goat anti-mouse horseradish peroxidase-conjugated (H+L) secondary antibody	Jackson ImmunoResearch Laboratories	Cat# 115-035-146 RRID: AB_2307392

(*Continued on next page*)

Continued

REAGENT or RESOURCE	SOURCE	IDENTIFIER
Mouse anti-rabbit horseradish peroxidase-conjugated (light chain specific) secondary antibody	Jackson ImmunoResearch Laboratories	Cat# 211-032-171 RRID: AB_2339149
Goat anti-mouse horseradish peroxidase-conjugated (light chain specific) secondary antibody	Jackson ImmunoResearch Laboratories	Cat# 115-035-174 RRID: AB_2338512
IRDye donkey anti-mouse 800CW	Li-Cor Biosciences	Cat# 925-32212 RRID: AB_2716622
IRDye donkey anti-rabbit 680RD	Li-Cor Biosciences	Cat# 925-68073 RRID: AB_2716687
Goat anti-rabbit biotinylated secondary antibody	Vector Laboratories	Cat# BA-1000 RRID: AB_2313606
Horse anti-mouse biotinylated secondary antibody	Vector Laboratories	Cat# BP-2000 RRID: AB_2687893
Streptavidin conjugated with Alexa Fluor 488	Invitrogen	Cat# S32354 RRID: AB_2315383
Goat anti-rabbit-Alexa Fluor 568	Invitrogen	Cat# A-11011 RRID: AB_143157
Bacterial and mammalian cell lines		
High efficiency DH5α cells	Invitrogen	Cat# 18258012
HEK-FT293	Invitrogen	Cat# R70007
AAV293	Cell Biolabs	Cat# AAV100
SH-SY5Y; RRID CVCL_0019	ATCC	Cat#CRL-2266
Recombinant DNA		
Rat enkephalin (ENK) promoter vector	Ferguson et al. 2011[50]	N/A
Rat dynorphin (DYN) promoter vector	Ferguson et al. 2011[50]	N/A
pLenti6.4V5DEST-CMV-sIRES-GFP	Ahmed, Berthet et al. 2010[35]	N/A
pcDNA3.0 vector	Invitrogen	Cat# V79020
pENTR vector	Invitrogen	Cat# A10462
pLenti6.4R4/R2 promoter less vector – Virapower High perform Promoterless gateway vector kit	Invitrogen	Cat# A11146
Virapower Lentivirus packaging mix	Invitrogen	Cat# K497500
RepCap5	Cell Biolabs	Cat# VPK425
pHelper plasmid from AAV helper free system	Agilent technologies	Cat# 240071
pLenti6.4 V5DEST-CMV-GFP-sIRES-Arrestin3-HA	Gurevich Laboratory, Department of Pharmacology, Vanderbilt University	N/A
pLenti6.4V5DEST -CMV-GFP-sIRES-Arrestin3(V343T)-HA	Gurevich Laboratory, Department of Pharmacology, Vanderbilt University	N/A
pLenti6.4V5DEST-CMV-T1A-YFP	Gurevich Laboratory, Department of Pharmacology, Vanderbilt University	N/A
pLenti6.4V5DEST-CMV-B1A-YFP	Gurevich Laboratory, Department of Pharmacology, Vanderbilt University	N/A
pLenti6.4 V5DEST-DYN-T1A-YFP	Gurevich Laboratory, Department of Pharmacology, Vanderbilt University	N/A
pLenti6.4 V5DEST-ENK-T1A-YFP	Gurevich Laboratory, Department of Pharmacology, Vanderbilt University	N/A
pLenti6.4V5DEST-DYN-Venus	Gurevich Laboratory, Department of Pharmacology, Vanderbilt University	N/A
pLenti6.4V5DEST-ENK-Venus	Gurevich Laboratory, Department of Pharmacology, Vanderbilt University	N/A

(*Continued on next page*)

Continued

REAGENT or RESOURCE	SOURCE	IDENTIFIER
Chemicals, peptides, and recombinant proteins		
6-OHDA	Sigma-Aldrich	Cat# 162957 CAS: 636-00-0
Desipramine hydrochloride	Sigma-Aldrich	Cat# D3900 CAS: 58-28-6
L-DOPA methyl ester	Sigma-Aldrich	Cat# D1507 CAS: 1421-65-4
Benserazide hydrochloride	Sigma-Aldrich	Cat# B7283 CAS: 14919-77-8
GFP magnetic agarose g beads	Chromotek	Cat# gtma
Lipofectamine 2000	Invitrogen	Cat# 11668027
Critical commercial assays		
Clonase LR II enzyme kit	Invitrogen	Cat# 11791020
iTaq Universal SYBR® Green Supermix	Bio-Rad	Cat#1725120
Purified arrestin-3	Vishnivetskiy et al., 2023[101]	N/A
Software and algorithms		
StatView	Abacus Corporation	N/A
Graphpad Prism Versions 9 and 10	Dotmatics	N/A

RESOURCE AVAILABILITY

Lead contact

Further information and requests for resources should be addressed to and will be fulfilled by the lead contact, Eugenia V. Gurevich (eugenia.gurevich@vanderbilt.edu).

Materials availability

This study generated new AAV and lentiviral vectors to express WT and mutant arrestin-3 proteins, Venus-tagged arrestin-3-derived JNK-activating peptide T1A, and homologous inactive arrestin-2-derived peptide B1A that can be obtained by researchers in not-for-profit organizations upon contacting the lead contact , Eugenia V. Gurevich (eugenia.gurevich@vanderbilt.edu).

Data and code availability

- All data reported in this paper will be shared by the lead contact upon request.
- Any additional information required to reanalyze the data reported in this work is available from the lead contact, Eugenia V. Gurevich (eugenia.gurevich@vanderbilt.edu), upon request.

EXPERIMENTAL MODEL AND STUDY PARTICIPANT DETAILS

Cell lines

SH-SY5Y human neuroblastoma cells (female) (ATCC CRL-2266), RRID: CVCL_0019.

Animals

Mice, C57Bl/6j (RRID: IMSR_JAX:000664), both sexes. Adult wild type (WT), Arr2 knockout (A2KO), and Arr3 knockout (A3KO) mice bred on a C57Bl/6j background (Charles River) were used. A2KO and A3KO mice were a generous gift from Dr. R. J. Lefkowitz (Duke University). The animals are housed at the Vanderbilt University animal facility in a 12/12 light/dark cycle with free access to food and water. The use of mice was approved by the Vanderbilt IACUC, protocol M1700093-00.

METHOD DETAILS

Virus construction and preparation

The full-length coding sequence of the bovine arrestin-3 (Arr3) (GI 6978467) (a.k.a. β-arrestin2) was N-terminally tagged with HA (Tyr-Pro-Tyr-Asp-Val-Pro-Asp-Tyr-Ala). The viral construct assembled in the lentiviral vector (LV) pLenti6.4/V5-DEST included GFP under control of the CMV promoter and downstream co-cistronic HA-tagged Arr3 under control of super-IRES (sIRES), which has been shown to significantly increase protein expression.[51] GFP alone was used as a control. The HA-tagged V343T mutant[40] and

Venus-tagged T1A[45] were produced by mutagenesis and verified by sequencing. The rat enkephalin (ENK) and dynorphin (DYN) promoter vectors were a gift from Dr. Neumaier (University of Washington).[50] The promoter sequences were inserted into the pLenti6.4/V5-DEST vector. The promoters were followed by sIRES before the coding sequence. The lentiviruses were produced using the ViraPower system (Invitrogen, Carlsbad, CA), concentrated and purified as described.[35] Viral titers of LVs with the CMV promoter were measured based on GFP or HA expression using HEK293 cells infected with the appropriate lentiviruses. The titers of lentiviruses with cell-specific promoters were determined by western blot for HIV1 p24 band using mouse monoclonal antibody (ThermoFisher). The adeno associated viruses serotype 5 (AAV5) encoding GFP (control) or HA-tagged Arr3 (with co-cistronic GFP) under control of the CMV promoter were constructed and produced using the AAV-DJ Helper Free Expression System and 293-AAV cell line (Cell Biolabs, Inc.). The viral titer was determined by standard qPCR with the BioRad SYBR Green supermix using serial dilutions of the cloning vector pAAV-MCS as standards.

Animal surgeries and virus injection

Mice were bred using heterozygous breeding pairs to obtain knockout and WT littermates. To maintain genetic homogeneity, mice were consistently backcrossed to WT C57Bl/6j mice from Charles River. The same WT animals were used for backcrossing of A2KO and A3KO mice to minimize background genetic differences. All procedures were performed in accordance with the NIH *Guide for the Care and Use of Laboratory Animals* and approved by the Vanderbilt University IACUC. The 6-OHDA lesion was performed essentially as described.[32,34] Briefly, mice were deeply anesthetized with ketamine/xylazine (100/10 mg/kg i.p.) and mounted on a stereotaxis. Mice were treated with desimipramine (25 mg/kg i.p.) for 20 min prior to infusion of 6-hydroxydopamine (6-OHDA). 6-OHDA (2 μL; 2 μg/μL solution in 0.05% ascorbic acid) was infused unilaterally into the medial forebrain bundle at coordinates AP = 1.1; ML = 1.3; H DV = 5.03. The mice were allowed to recover for 4 weeks after surgery. The viruses encoding Arr3 or Arr3-derived peptides (or GFP control) were injected 24 h after the end of the behavioral pre-testing. The mice were anesthetized with ketamine/xylazine (100/10 mg/kg i.p.) and mounted on a stereotaxis. The virus injection (3 μL of the concentrated virus in saline per striatum at 0.3 μL/min) was made unilaterally (on the 6-OHDA-lesioned side) into the dorso-lateral posterior CPu, the region critical for the development of behavioral manifestations,[30,31,102,103] at coordinates AP +1.02; ML 1.65; DV 3.55. In the experiments performed to test for the DYN and ENK promoters' specificity, 2 μL of lentiviruses encoding GFP under control of the DYN or ENK promoters were injected bilaterally into the globus pallidus (GP) at coordinates AP = −0.46; ML = ±0.90; DV = 4.00 or into the substantia nigra pars compacta at coordinates AP = −3.08; ML = ±1.40; DV = 4.60.

Animal behavior

Rotations

Four weeks after the 6-OHDA lesion, the animals were tested for rotational response to apomorphine (0.1 mg/kg s.c.) for 1 h using an automated rotometer (AccuScan Instruments). Both ipsilateral and contralateral 360° turns were recorded, and the net rotational asymmetry (contralateral minus ipsilateral turns) was calculated. The animals were then treated, starting the next day, with L-DOPA (L-3,4-Dyhydroxyphenylalanine methyl ester hydrochloride, 25 mg/kg i.p. twice daily, morning and afternoon) for 4–5 days, and the rotational response was recorded every day after the morning injection (pre-testing). After the pre-testing, the A3KO and WT mice were both separated into groups according to the number of rotations on the last day of pre-testing, and members of each group were randomly assigned to the experimental groups to receive the appropriate viruses. This randomization procedure served to equalize the experimental groups and reduce variability, allowing us to minimize the number of animals needed to achieve significant results. The virus injection was made on the next day after the last pre-testing session. Five days after the injection of lentiviruses or 3 weeks after the AAV injection, the mice were again treated with L-DOPA (25 mg/kg i.p. twice daily) and tested for L-DOPA-induced rotations every day for 10 days, as described.[35,56]

Abnormal involuntary movements

Testing for abnormal involuntary movements (AIMs) was performed essentially as described.[35] The mice were treated with increasing doses of L-DOPA (1–10 mg/kg day) for 15 days, starting 4 weeks after the 6-OHDA lesion. The L-DOPA dose during pre-testing increased from session to session from 1 mg/kg to 6 mg/kg, s.c., with the 6 mg/kg dose used in the last pre-testing session. This is done to increase the rate of AIMs by the end of the pre-testing to facilitate the scoring procedure during post-testing. All mice of both genotypes received the same dose of L-DOPA in each session either the same as in the last pre-testing session or higher if needed. The dose adjustment during pre-testing and randomization procedure based on the pre-testing scores similar to that used for rotations served to equalize the experimental groups, reduce variability and allowed to minimize the number of animals needed to achieve significant results. After the pre-testing, the A3KO or WT mice each were grouped according to their AIMs score, and members of each group were randomly assigned to the experimental groups to receive appropriate viruses. The virus injection was performed on day 14, and the mice were allowed to recover for 5 days (all LV experiments) or 3 weeks (the LV-AAV experiment) before resuming the treatment for 18 more days with 6–10 mg/kg L-DOPA. During the testing period, all animals received the same dose of L-DOPA in all sessions. Depending on the AIMs scores achieved during pre-testing, the dose either remains at 6 mg/kg s.c., or was further increased to 10 mg/kg, s.c. AIMs were assessed by an independent observer in a blind manner using a 0–4 scale[104] on every third day, as described.[35,56] Briefly, the AIMs were scored by an independent observer unaware of the animal's experimental status on 0–4 scale: 0 – no AIMs; 1 – infrequent AIMs occurring <50% of the time; 2 – frequent AIMs occurring >50% of the time; 3 – constantly present AIMs that are interrupted by external stimulation (tap on the cage); 4 – constant AIMs that are insensitive to

external stimulation. Four types (orolingual, limb, locomotor, and axial) of AIMs were assessed every 20 min for 1 min during a 3-h session every third day (total 9 observations; maximal score for each observation 16, maximal total score per session 144).

Cylinder test

The cylinder test was performed as described.[35] Half of the WT and A3KO mice were randomly selected to receive injections of L-DOPA (6 mg/kg, s.c.); the other half received saline. The mice were placed in a glass cylinder close to a mirror and their behavior was video recorded under a red light for 6 min. The behavior was scored from videotapes by an independent observer blind to the mouse genotype, experimental condition, and the side of the lesion. The next day, the treatment groups were switched. The number of times a mouse used the contralateral (injured) or ipsilateral paw for support was counted from the recordings by an observer blind to the animal's treatment (use is defined as the animal supporting its body with digits extended). Preferential use of the paw ipsilateral to the lesion (controlled by the intact hemisphere) is indicative of the akinetic defect of the lesion. Acute L-DOPA administration enhances the use of the contralateral paw, controlled by the lesioned hemisphere.[28,105,106] The results are expressed as a percentage of contralateral paw usage relative to the ipsilateral paw.

Tissue preparation

Upon completion of the drug administration and behavioral testing, the mice were anesthetized with isoflurane, decapitated, the brains were collected and rapidly frozen on dry ice. The midbrain containing the substantia nigra was dissected and post-fixed in 4% paraformaldehyde for tyrosine hydroxylase (TH) immunohistochemistry to determine the loss of dopaminergic neurons. The rostral parts of the brains containing the striata were kept at −80°C until samples were collected for western blot analysis. To collect the samples for western blot, the brains were cut through the striatum, the position of the virus injection track was identified, and the tissue around the injection track was collected to determine the expression of virus-encoded proteins and TH level, as described previously.[35,56] Randomly selected animals were overdosed with ketamine/xylazine and transcardially perfused with 4% paraformaldehyde. The brains were removed, post-fixed in 4% paraformaldehyde, cryoprotected, kept frozen at −80°C, then cut into 30 μM sections and used for immunohistochemistry. The mice used for testing the DYN/ENK promoters' specificity were treated in the same manner in preparation for immunohistochemistry.

Western blot

To determine the lesion quality, we used western blot of the striatal tissue for TH with rabbit anti-TH antibody (Chemicon, AB152; 1:10,000 dilution). The expression of GFP- or Venus-tagged constructs was measured by western blot with mouse anti-GFP antibody (Clontech; 1:2,000). The expression of WT and mutant arrestin-3 was measured with rabbit polyclonal anti-arrestin-3 antibody, as described.[34] To detect HA-tagged constructs, rabbit monoclonal anti-HA antibody (Cell Signaling, cat # 3724; 1:1,000) was used. Active JNK was detected with rabbit antibodies to doubly phosphorylated (Thr183/Tyr185) JNK (Cell Signaling, catalog # 4668 or 9251; 1: 1,000). c-Jun phosphorylated at the JNK phosphorylation site Ser73 was detected with a phospho-specific rabbit antibody (Cell Signaling, # 3270; 1:1,000) and the total c-Jun – with mouse monoclonal antibody (Cell Signaling, # 2315; 1:1,000). Doubly phosphorylated (active) ERK1/2 was detected with a phospho-ERK-specific [phosphor-ERK1/2(Thr202/Tyr204)] mouse monoclonal antibody (Cell Signaling, # 9106) at 1:2,000 dilution. After stripping, blots were re-probed with a rabbit anti-ERK1/2 antibody (Cell Signaling, # 9102) at 1:1,000 dilution to detect total ERK1/2. Akt phosphorylated at Thr308 was visualized with rabbit anti-Akt(T308) antibody (Cell Signaling, # 9275), phosphorylated at Ser473 - with anti-Akt(S473) rabbit antibody (Cell Signaling, # 4060), and total Akt was detected with a rabbit antibody (Cell Signaling, # 9272), all at 1:1,000 dilution. Phospho-p38 was detected with a rabbit monoclonal antibody (Cell Signaling, # 4511; 1:1,000) and total p38 – with a rabbit antibody (Cell Signaling, # 9212, 1:1,000). Anti-rabbit or anti-mouse horseradish peroxidase-conjugated secondary antibodies (Jackson Immunoresearch) were used at 1:10,000 dilution. The blots were developed with a chemiluminescent substrate and either exposed to X-ray film or subjected to direct detection using C-DiGit Blot scanner (Li-Cor). The gray values of the bands on X-ray film were measured with a Versadoc imaging system (Bio-Rad) with QuantityOne software. Following direct detection, Image Studio software was used. Fluorescent detection of the peptide expression combined with TH and the marker of medium spiny neurons forkhead box P1 (FOXP1)[107] was performed with mouse anti-GFP antibody (1:1,000), rabbit anti-TH (1:1,000) and rabbit anti-FOXP1 (1:500) followed by IRDye donkey anti-mouse 800CW (green) and donkey anti-rabbit 680 (red) antibodies (Li-Cor) at 1:10,000 dilution. The blots were imaged with the Odyssey Clx system and analyzed with Image Studio software.

Immunohistochemistry

The lesion quality was tested by tyrosine hydroxylase (TH) immunohistochemistry. The midbrain sections containing the substantia nigra were stained with rabbit anti-TH antibody (Chemicon, Temecula, CA; 1:1,000 overnight at 4°C) followed by anti-rabbit secondary antibody conjugated with Alexa 594 (red).

To detect the expression of GFP-tagged constructs by immunohistochemistry, the mouse monoclonal anti-GFP (JL-8, Clontech; 1:500 overnight at 4°C) primary antibody was used, followed by goat anti-rabbit biotinylated secondary antibody and streptavidin conjugated with Alexa Fluor 488 (Invitrogen, Carlsbad, CA). For double labeling with FOXP1, the sections were labeled with mouse anti-GFP (1:500) antibody and rabbit anti-FOXP1 antibody (Cell Signaling Technology; 1:400) and detected by biotinylated secondary antibody/streptavidin-Alexa Fluor 488 (GFP; green) and anti-rabbit-Alexa Fluor 568 (FOXP1; red). Alternatively, chicken anti-GFP

antibody (Invitrogen; 1:500) was used. For double labeling with TH, the sections were labeled with mouse anti-GFP (1:500) antibody and rabbit anti-TH antibody (Chemicon; 1:1000) and detected by biotinylated secondary antibody/streptavidin-Alexa Fluor 488 (GFP; green) and anti-rabbit-Alexa Fluor 568 (TH; red). Double labeling for phospho-*c*-Jun and TH was performed with phospho-specific rabbit monoclonal antibody (Cell Signaling, # 3270; 1:500) for c-Jun and sheep anti-TH antibody (Novex Biotechnology; 1:400), biotinylated secondary antibody/streptavidin-Alexa Fluor 488 (phospho-*c*-Jun; green) and anti-rabbit-Alexa Fluor 568 (TH; red). The sections were photographed at low magnification on a Nikon TE2000-E automated microscope with a 4× dry objective and an Andor Zyla high resolution digital camera using the stitching function of the Nikon NIS-Elements software. High power photographs were collected on an Olympus FV-100 confocal microscope in the green and red channels with z-sectioning using a 40× oil immersion objective at 1024× 1024 pixels. The images were assembled in Photoshop, with minimal contrast adjustments applied separately to channels to equalize their intensity.

In-cell JNK phosphorylation assay

Human neuroblastoma SH-SY5Y cells were cultured in DMEM/F12 media supplemented with 10% fetal bovine serum and 1% penicillin/streptomycin. Cells were co-transfected with HA-tagged JNK3α2 and with either: (1) empty vector; (2) WT arrestin-3; or (3) arrestin-3-V343T mutant. Similarly, in the T1A experiment, the cells were transfected with HA-JNK3α2 and with half or full concentration of WT Venus-tagged-ARR3, half or full concentration of Ve-T1A, or full concentration of Ve-B1A. In the arrestin-3 dose-response experiment, the cells were transfected with increasing concentrations of WT arrestin-3. Activation of JNK3 was assessed by western blot with a ppJNK specific antibody (Cell Signaling, # 9251 or 4668), as described.[45,108,109] To detect the JNK3 expression, JNK3-specific mouse (Santa Cruz Biotechnology) or rabbit anti-HA antibody (Cell Signaling, # 3724) was used. Arr3 and Arr3-derived constructs were detected with rabbit anti-Arr3[34] or mouse anti-GFP (Clontech JL-8) antibody. Total JNK level was measured with rabbit anti-SAPK/JNK antibody (Cell Signaling technology, # 9152).

Immunoprecipitation from the striatal tissue

The lesioned and intact striata from 6-OHDA-lesioned WT and A3KO mice chronically treated with L-DOPA and challenged with an L-DOPA dose 45 min before sacrifice were dissected and lysed in NP-40-containing immunoprecipitation (IP) buffer, as described.[72,110] The lysates were cleared by centrifugation, equalized by protein content with IP buffer, and the supernatants were incubated overnight at 4°C with rabbit anti-JNK3 antibody (Cell Signaling). Protein G slurry (20 μL) was added to each tube, and incubation was carried out at 4°C for 2 h. The resin was washed 3 times with IP buffer, and samples were eluted with SDS buffer. Samples were analyzed by western blot with rabbit anti-ppJNK (Cell Signaling Technology, #4668) and rabbit anti-JNK3 (Cell Signaling Technology, #2305) antibodies.

QUANTIFICATION AND STATISTICAL ANALYSIS

The rotation data were real numbers measured automatically. Therefore, the rotation numbers were analyzed by parametric two-way repeated measure ANOVA with Group (GFP versus Arr3, Arr3 mutant, Venus-T1A, or Venus-B1A peptide) as a between group and Day as a repeated measure factor (as a measure measured repeatedly in the same animal). The group differences across sessions were assessed by the post hoc Bonferroni/Dunn, Tukey, or by Dunnett's test (with correction for multiple comparisons) where appropriate. When a significant effect of Group was observed, the data for individual sessions were compared by the unpaired Student's test (two groups) or by the Bonferroni/Dunn post hoc test with correction for multiple comparisons, when appropriate.

The AIMs scores were assessed by a human observer blind to the animals' genotypes and experimental conditions. As scores, these measures are inherently non-parametric and were, therefore, analyzed by nonparametric statistics. AIMs scores for each session were compared by Kruskal-Wallis non-parametric ANOVA followed by Dunn's post hoc test with correction for multiple comparisons. The data for the cylinder test were analyzed using the nonparametric paired Wilcoxon Signed Rank test (to evaluate the effect of L-DOPA) or the Mann-Whitney test (for group comparison).

The signaling data (active ERK1/2, Akt and p38) were analyzed by three-way ANOVA with Genotype (WT versus A3KO) and Challenge (L-DOPA versus saline injection) as between group and Hemisphere (Intact versus Lesioned) as within group factors. The results of JNK3 immunoprecipitation and c-Jun phosphorylation experiments were similarly analyzed by three-way ANOVA with Genotype (WT versus A3KO) and Challenge (L-DOPA versus saline injection) as between group and Hemisphere (Intact versus Lesioned) as within group factors. The data on the rescue of the JNK3 activity or c-Jun phosphorylation in the lesioned striata were analyzed by one-way ANOVA with Genotype as main factor followed by Bonferroni's post hoc comparison of means. The data on the expression of HA-Arr3 or Venus-T1A were analyzed by unpaired Student's t test; the expression of endogenous Arr3 in the intact and lesioned hemispheres was compared by paired Student's t test.

StatView (SAS Institute) and Prism GraphPad software were used for the statistical analysis. The value of $p < 0.05$ was considered significant.